



Ground-based  
aerosol climatology  
of China

H. Che et al.

This discussion paper is/has been under review for the journal Atmospheric Chemistry and Physics (ACP). Please refer to the corresponding final paper in ACP if available.

# Ground-based aerosol climatology of China: aerosol optical depths from the China Aerosol Remote Sensing Network (CARSNET) 2002–2013

H. Che<sup>1</sup>, X. Zhang<sup>1</sup>, X. Xia<sup>2</sup>, P. Goloub<sup>3</sup>, B. Holben<sup>4</sup>, H. Zhao<sup>5</sup>, Y. Wang<sup>1</sup>, X. Zhang<sup>6</sup>, H. Wang<sup>1</sup>, L. Blarel<sup>4</sup>, B. Damiri<sup>7</sup>, R. Zhang<sup>8</sup>, X. Deng<sup>9</sup>, Y. Ma<sup>5</sup>, T. Wang<sup>10</sup>, F. Geng<sup>11</sup>, B. Qi<sup>12</sup>, J. Zhu<sup>2</sup>, J. Yu<sup>13</sup>, Q. Chen<sup>13</sup>, and G. Shi<sup>14</sup>

<sup>1</sup>Key Laboratory of Atmospheric Chemistry (LAC), Chinese Academy of Meteorological Sciences (CAMS), CMA, Beijing, 100081, China

<sup>2</sup>Laboratory for Middle Atmosphere and Global Environment Observation (LAGEO), Institute of Atmospheric Physics, Chinese Academy of Sciences, Beijing, 100029, China

<sup>3</sup>Laboratoire d'Optique Atmosphérique, Université des Sciences et Technologies de Lille, 59655 Villeneuve d'Ascq, France

<sup>4</sup>Biospheric Sciences Branch, Code 923, NASA/Goddard Space Flight Center, Greenbelt, MD, USA

<sup>5</sup>Institute of Atmos. Environ., China Meteorological Administration, Shenyang 110016, China

<sup>6</sup>Meteorological Observation Center, CMA, Beijing, 100081, China

Title Page

Abstract

Introduction

Conclusions

References

Tables

Figures



Back

Close

Full Screen / Esc

Printer-friendly Version

Interactive Discussion



<sup>7</sup>Cimel électronique, Paris, 75011, France

<sup>8</sup>Key Laboratory of Regional Climate-Environment for Temperate East Asia (RCE-TEA), Institute of Atmospheric Physics, Chinese Academy of Sciences, Beijing 100029, China

<sup>9</sup>Institute of Tropical and Marine Meteorology/Guangdong Provincial Key Laboratory of Regional Numerical Weather Prediction, CMA, Guangzhou 510080, China

<sup>10</sup>School of Atmospheric Sciences, Nanjing University, Hankou Rd. 22, Nanjing 210093, China

<sup>11</sup>Shanghai Urban Environmental Meteorology Center, Pudong New Area Weather Office, SMB, Shanghai 200135, China

<sup>12</sup>Hangzhou Meteorological Bureau, Hangzhou 310051, China

<sup>13</sup>Plateau Atmospheric and Environment Key Laboratory of Sichuan Province, College of Atmospheric Sciences, Chengdu University of Information Technology, Chengdu 610225, China

<sup>14</sup>State Key Laboratory of Numerical Modeling for Atmospheric Sciences and Geophysical Fluid Dynamics (LASG), Institute of Atmospheric Physics, Chinese Academy of Sciences, Beijing, 100029, China

Received: 20 March 2015 – Accepted: 15 April 2015 – Published: 29 April 2015

Correspondence to: H. Che (chehz@cams.cma.gov.cn)

Published by Copernicus Publications on behalf of the European Geosciences Union.

**Ground-based  
aerosol climatology  
of China**

H. Che et al.

Title Page

Abstract

Introduction

Conclusions

References

Tables

Figures



Back

Close

Full Screen / Esc

Printer-friendly Version

Interactive Discussion



## Abstract

Long-term measurements of aerosol optical depths (AOD) and Angstrom exponents (Alpha) made for CARSNET were compiled into a climatology of aerosol optical properties for China. Quality-assured monthly mean AODs are presented for 50 sites representing remote, rural, and urban areas. AODs were 0.14, 0.34, 0.42, 0.54, and 0.74 at remote stations, rural/desert regions, the Loess Plateau, central and eastern China, and urban sites, respectively, and the corresponding Alpha values were 0.97, 0.55, 0.82, 1.19, and 1.05. AODs increased from north to south, with low values ( $< 0.20$ ) over the Tibetan Plateau and northwestern China and high AODs ( $> 0.60$ ) in central and eastern China where industrial emissions and anthropogenic activities were likely sources. AODs were 0.20–0.40 in semi-arid and arid regions and some background areas in north and northeast China. Alphas were  $> 1.20$  over the southern reaches of the Yangtze River and at clean sites in northeastern China. In the northwestern deserts and industrial parts of northeast China, Alphas were lower ( $< 0.80$ ) compared with central and eastern regions. Dust events in spring, hygroscopic particle growth during summer, and biomass burning contribute the high AODs, especially in northern and eastern China. The AODs show decreasing trends from 2006 to 2009 but increased  $\sim 0.03 \text{ yr}^{-1}$  from 2009 to 2013.

## 1 Introduction

Aerosol particles are important for global and regional climate because particulate matter (PM) can scatter or absorb solar radiation, depending on the particles' composition, size, etc. (Charlson et al., 1992) and cause either large-scale cooling or warming (Hansen et al., 1997). Despite the numerous studies that have been conducted in recent years, aerosol optical properties are still one of the largest sources of uncertainty in current assessments and predictions of global climatic change (IPCC, 2013, 2007; Hansen et al., 2000; Ramanathan et al., 2001).

**Ground-based  
aerosol climatology  
of China**

H. Che et al.

Title Page

Abstract

Introduction

Conclusions

References

Tables

Figures



Back

Close

Full Screen / Esc

Printer-friendly Version

Interactive Discussion



Satellite monitoring and ground-based observations are two important ways for monitoring the Earth's aerosol properties long-term (Holben et al., 2001). Ground-based measurement networks are especially useful for validating and augmenting remotely-sensed data (Holben et al., 2001). So far several automatic robotic ground-based networks have been established; these include the Cimel sunphotometer based networks of AERONET (Holben et al., 1998), PHOTONS (Goloub et al., 2008), AEROCAN (Bokoye et al., 2001), RIMA (Prats et al., 2011), the skyradiometer network (SKYNET, Kim et al., 2004; Uchiyama et al., 2005), the WMO GAWPFR Network (Wehrli, 2002), and so on. Information on aerosol optical properties obtained from these networks contribute to our understanding of the earth's systems because it can be used to (1) characterize the ambient aerosol, (2) address larger questions concerning environmental pollution, (3) validate satellite retrievals and numerical modeling algorithms, and (4) investigate aerosol and cloud effects on radiative fluxes (Holben et al., 2001).

China is the most populated and largest developing country in the world, and it has become one of the largest global sources for aerosol particles and their precursors due to the copious industrial emissions and frequent dust events (Huebert et al., 2003; Seinfeld et al., 2004; Li et al., 2007). These aerosol particles not only affect the local atmospheric environment but also are transported to the East Asia and Pacific regions and beyond (Streets et al., 2001; Eck et al., 2005) where the transported materials can cause significant effects on regional weather and climate and also human health (Che et al., 2005; Liang and Xia, 2005; Xia, 2010; Chen et al., 2011).

Ground-based sunphotometers were first used to retrieve aerosol optical data in China in the early 1980s (Zhao et al., 1983; Qiu et al., 1983; Mao et al., 1983). Since then, there have been many investigations into aerosol optical properties, and studies have been conducted in north China, northeast China, Tibet Plateau, northwest desert region and eastern coast region of China, etc. (Wang and Qiu, 1988; Li et al., 1995; Hu et al., 2001; Zhang et al., 2002; Xia et al., 2005; Tan et al., 2009). These studies have provided valuable information on local aerosol optical properties, but they were carried at different times with different instruments, and more often than not, used different cal-

**Ground-based  
aerosol climatology  
of China**

H. Che et al.

Title Page

Abstract

Introduction

Conclusions

References

Tables

Figures



Back

Close

Full Screen / Esc

Printer-friendly Version

Interactive Discussion



ibration procedures, calculation algorithms, and so forth. This lack of standardization has made it difficult to characterize regional and temporal variations in aerosol optical properties. Accordingly, Qiu et al. (1998) and Qin et al. (2010) proposed methods to retrieve AOD based on surface-based broadband solar radiation and horizontal visibility observation data. Long-term measurements of AODs and their distributions were retrieved in China from 1960s to 2000s (Qiu and Yang, 2000; Luo et al., 2001; Qin et al., 2010).

Ground-based networks for measuring aerosol optical properties in China were first established in the 1990s. Zhang et al. (2002) studied aerosol optical properties at four sites – Miyun, Xinfeng, Waliguan, and Dangxiong. Several SKYNET sites including Dunhuang, Yinchuan, Beijing, Qingdao, and Hefei in northern China were established from 1997 (Kim et al., 2004). At present, SKYNET has expanded to 10 sites in China, and a series of studies on optical properties and radiative forcing over different regions in China has been undertaken for that program (Kim et al., 2005; Che et al., 2008, 2014; Liu et al., 2009; Wang et al., 2014). Another network, the Chinese Sun Hazemeter NETWORK (CSHNET) includes 24 stations established in 2004 to measure aerosol optical properties and their spatial and temporal variations throughout the China. Hand-held sunphotometers have been used for that program (Xin et al., 2007). AERONET/PHOTONS established four sites in Beijing and Yulin beginning in 2001, (Alfaro et al., 2003; Fan et al., 2006; Che et al., 2009c), and there are now ~ 40 AERONET and PHOTONS sites in China ([http://aeronet.gsfc.nasa.gov/cgi-bin/type\\_piece\\_of\\_map\\_opera\\_v2\\_new](http://aeronet.gsfc.nasa.gov/cgi-bin/type_piece_of_map_opera_v2_new)); and the data from those sites have been widely used (Xia et al., 2005; Li et al., 2007; Mi et al., 2007; Eck et al., 2010; Bi et al., 2011). However, observations at most of these sites were only for field-campaigns, and only several sites have data records long enough to characterize seasonal variations in aerosol optical properties (Zhu et al., 2013; Fan et al., 2015). Indeed, the existing data are inadequate for a comprehensive evaluation of aerosol properties in China (Eck et al., 2005).

**Ground-based  
aerosol climatology  
of China**

H. Che et al.

Title Page

Abstract

Introduction

Conclusions

References

Tables

Figures



Back

Close

Full Screen / Esc

Printer-friendly Version

Interactive Discussion



The China Aerosol Research Network (CARSONET) is a ground-based network for monitoring aerosol optical properties, and it uses the same types of instruments as AERONET (Che et al., 2009a). CARSONET includes 20 sites located north and north-west China that were first established by the China Meteorological Administration (CMA) in 2002 for dust aerosol monitoring. This network has increased to more than 60 stations that are now operated not only by CMA but also by local meteorological administrations, institutes, and universities throughout China. This has become a national resource for studying aerosol optical properties over the different regions in China and for validating satellite retrievals and numerical models of aerosols (Xie et al., 2011; Zhao et al., 2013a; Che et al., 2014; Lin et al., 2014).

The primary objective of this paper is to present a climatology of aerosol optical properties developed from CARSONET measurements made from 2002 to 2013. This study characterizes the spatial and temporal variations of aerosol optical properties using data from 50 CARSONET sites with at least one year of measurements. Remote, rural and urban regions of China are all represented in the study. The contents of this article include: (1) a description of the sites, data processing, and data quality control, (2) an evaluation of the spatial characteristics of AOD and Angstrom exponent over different regions of China, and (3) an analysis of the monthly AODs at 440 nm and the Angstrom exponents between 440 to 870 nm (Alpha) at all 50 sites, (4) a discussion of the long-term (12 yr) variations of AOD at 12 CARSONET sites. To provide a record of CARSONET results, monthly and yearly average AODs and Alphas for the 50 CARSONET sites are provided as Appendix tables. We hope this database will be used for future investigations of aerosols, climate, and the atmospheric environment of China.

## 2 Site description, instruments, and data

### 2.1 Site descriptions

As shown in Fig. 1 and described in detail in the Appendix tables, Cimel sun photometers (Cimel Electronique, CE-318) were installed at 50 CARSNET sites between 2002 to 2013. The stations can be classified into three general groups: remote, rural, and urban. The four remote stations were set up on Tibet Plateau (> 3000 m a.s.l.) and at regional background site in northwest China, and all these sites are far from anthropogenic influences. The twenty-five rural sites were selected to be representative of areas relatively unaffected by local sources and well above the surrounding ground surface. The rural sites can be further classified as sites representing (a) desert regions (eleven sites), which are mainly affected by dust aerosol particles with relatively small anthropogenic influences, (b) the Loess Plateau (four sites) which are affected not only by dust but also by more anthropogenic activities than the nearby desert rural sites, (c) central and eastern China (ten sites) which are more strongly affected by anthropogenic activities and are located near or surrounded by large cities, and (d) urban sites (twenty-one sites) located in the centers or heavily populated areas of cities, many of which are provincial capitals.

### 2.2 Instruments and calibration

Cimel sun photometers were deployed at each CARSNET site. These instruments make direct spectral solar radiation measurements in a  $1.2^\circ$  full field-of-view every 15 min (Holben, 1998). Because the network has been expanded from the original 20 sites to 50 sites at present, several different types of Cimel instruments have been used; these include: (1) logical type at five normal wavelengths of 440, 675, 870, 940, and 1020 nm and three polarization bands at 870 nm, (2) numerical type at five normal wavelengths of 440, 675, 870, 940, and 1020 nm and three polarization bands at 870 nm, (3) numerical type at eight wavelengths of 340, 380, 440, 500, 675, 870,

Title Page

Abstract

Introduction

Conclusions

References

Tables

Figures



Back

Close

Full Screen / Esc

Printer-friendly Version

Interactive Discussion



**Ground-based  
aerosol climatology  
of China**

H. Che et al.

Title Page

Abstract

Introduction

Conclusions

References

Tables

Figures



Back

Close

Full Screen / Esc

Printer-friendly Version

Interactive Discussion



940, and 1020 nm, (4) and numerical type at nine wavelengths of 340, 380, 440, 500, 675, 870, 940, 1020 and 1640 nm. Measurements at 340, 380, 440, 500, 675, 870, 1020, and 1640 nm were used to retrieve AODs, and measurements at 940 nm were used to obtain the total precipitable water content in centimeters (Brent et al., 1998; Dubovik et al., 2000a). The total uncertainty in the AODs is about 0.01 to 0.02 (Eck et al., 1999). Aerosol size distributions, refractive indices, and single-scattering albedos were retrieved by using sky radiance almucantar measurements and direct sun measurements following the procedures described in Dubovik et al. (2000b, 2006).

Five CARSNET master quality sunphotometers were calibrated using the Langley method at the either the Izaña, Spain (28.31° N, 16.50° W, 2391.0 m a.s.l.) or the Mauna Loa, USA (19.54° N, 55.58° W, 3397.0 m a.s.l.) global observatories which are the master calibration sites for PHOTONS (also RIMA) and AERONET. These reference instruments were typically re-calibrated at Izaña every 6 months. These master instruments were then installed at the Beijing-CAMS site (39.93° N, 116.32° E, 106.0 m a.s.l., which is operated for both CARSNET and AERONET), and they were used to inter-calibrate all field CARSNET instruments at least once a year following the AERONET calibration protocol (Che et al., 2009a).

The requirements for inter-comparison calibration protocol for the CARSNET field instruments were as follows: (a) only raw data collected from 2.00 to 6.00 a.m. (GMT + 08:00) on clean and clear days were used, (b) the AODs at 500 nm on calibration days had to be less than 0.20 and without major fluctuations, (c) the time intervals between the measurements made with two masters and the instruments to be calibrated had to be less than 10 s. The AODs obtained from un-calibrated instruments differed by 4.5 to 15.3% compared with those measured by reference instruments. After the calibration with the master instruments, however, the daily average AODs differed by < 1.5% relative to the master measurements (Che et al., 2009c). According to Brent et al. (1998), yearly calibrations of the field instruments ensured the accuracy of the CARSNET measurements, and therefore, the AODs from the 50 CARSNET stations were of high quality and reliable.

**Ground-based  
aerosol climatology  
of China**

H. Che et al.

[Title Page](#)[Abstract](#)[Introduction](#)[Conclusions](#)[References](#)[Tables](#)[Figures](#)[Back](#)[Close](#)[Full Screen / Esc](#)[Printer-friendly Version](#)[Interactive Discussion](#)

The sphere calibration methods and protocols for CARSNET have been described by Tao et al. (2014). The CARSNET sphere calibration results differed from the original values provided by the manufacturer, Cimel Electronique, S.A.S., by  $\sim 3\text{--}5\%$  at infrared wavelengths (1020 and 870 nm) and  $\pm 3\%$  at visible wavelengths (440, 500, and 675 nm). Similar to Brent et al. (1998), sphere calibrations of all CARSNET field instruments were done annually to ensure the accuracy of the sky irradiance measurements.

### 2.3 Data processing and quality control

The AODs were calculated using the ASTPwin software provided by the manufacturer of the sunphotometers. This software can provide Level 1.0 AOD (raw results without cloud-screening), Level 1.5 AOD (cloud-screened AOD based on the work of Smirnov et al., 2000) and Angstrom Exponents (Alpha) between 440 to 870 nm. For the present study, all AOD data were computed by interpolation of the inter-calibration coefficients, and the cloud-screened AOD based on the method of Smirnov et al. (2000) also were obtained. We note that the cloud-screening technique has not been completely validated although the procedure tested favorably using experimental data obtained under different geographical and optical conditions (Smirnov et al., 2000). To further ensure the data quality, all the data were checked manually site-by-site, and any unreasonable data were deleted. For example, some exceptionally large AOD points were caused by the clouds, and this was determined after checking the MODIS Level-1B granule (MOD02\_1km) images, which are available from <http://modis-atmos.gsfc.nasa.gov/IMAGES/>. Daily average AODs were the first values computed, and any cases where measurements were made less than 10 times in a day were eliminated. This processing procedure eliminated  $\sim 20\%$  of the daily data. Finally, the monthly and yearly averages of the AODs were calculated at each wavelength as were the Angstrom exponents between 440 and 870 nm.

Che et al. (2009) validated AODs from CARSNET-CAMS stations through comparisons with data from the AERONET stations in Beijing. A comparison between

**Ground-based  
aerosol climatology  
of China**

H. Che et al.

[Title Page](#)[Abstract](#)[Introduction](#)[Conclusions](#)[References](#)[Tables](#)[Figures](#)[Back](#)[Close](#)[Full Screen / Esc](#)[Printer-friendly Version](#)[Interactive Discussion](#)

the AODs calculated by ASTPWin procedure vs. AERONET results, showed that the ASTPWin AOD values were about 0.03, 0.01, 0.01, and 0.01 larger than those from AERONET at 1020, 870, 670, and 440 nm, respectively. Thus, the sets of results from two networks were very consistent with one another as the correlation coefficients were larger than 0.999 and had a 99.9 % significance level. Synchronous observations also were compared between two nearby Yangtze River delta region sites, one at the AERONET Zhejiang Forest University site and the other the Lin'an regional CARSNET background site (Pan et al., 2011). The differences of AOD in that comparison were less than 0.02, which again indicates similar accuracies in the results from CARSNET and AERONET.

### 3 Results: CARSNET measurements

#### 3.1 Spatial distributions of aerosol optical properties in China

##### 3.1.1 Spatial distributions of AOD and Alpha

The spatial distribution of AOD (Fig. 2a) and Alpha (Fig. 2b) based on data obtained from the CARSNET stations are shown in Fig. 2. In general, the AODs increased from north to south (Fig. 2a). Low AODs ( $< 0.20$ ) occurred at remote stations, that is, Mt. Waliguan, Shangri-La, and Lhasa on the Tibetan Plateau at altitudes  $> 3000$  m a.s.l. and at Akedala in a remote region of northwestern China. All of the remote sites are subject to only minimal anthropogenic influences, and the aerosol loadings are very low because of this (Zhang et al., 2012). Large AODs ( $> 0.60$ ) mainly occurred in central and eastern China, especially regions with strong anthropogenic influences in the northeastern plain, north China plain, Yangtze River delta, Pearl River delta, Sichuan basin, and Guanzhong plain (Zhang et al., 2012). Several sites in northwestern China also showed AOD  $> 0.60$ ; these include the urban site at Lanzhou and desert-margin site at Hotan, Xinjiang Province. AODs from 0.20–0.40 occurred in semi-arid and arid

regions of north China and some regional background sites such as Mt. Tai – the background site for the north China plain and Mt. Longfeng – the background site on the northeast China plain.

From Fig. 2b, we can see that the spatial distribution of Alpha in China also shows clear variability, for example large Alpha ( $> 1.20$ ) were found along the southern reaches of the Yangtze River and at clean sites of northeastern China; this shows that the aerosol particles in these areas are smaller than in most other regions of China. In the desert regions of northwestern China and industrial region of northeastern China, the Alpha values were considerably lower ( $< 0.80$ ) than those of central and eastern regions such as North China Plain, Guanzhong Plain and Sichuan Basin (Alpha  $> 0.80$ ). The Alpha values were  $\sim 0.60$ – $0.80$  in arid regions of northern China. In particular, the Alphas were typically  $< 0.40$  in the Taklimakan desert region (e.g., Tazhong and Hotan) which suggests that large mineral dust particles were major components of the aerosol populations in this region (Che et al., 2013).

Figure 3 shows the spatial distributions of AOD and Alpha separately for each of the four seasons. Of the 50 CARSNET sites, 27 had AODs  $< 0.60$  in spring and summer compared with 32 in the fall and 30 in winter (Fig. 3a–d), and this shows that the aerosol extinctions of China were generally larger in spring and summer compared with fall and winter. Moreover, most of the sites with AODs  $< 0.60$  were located in northern China. In southern China, AODs  $< 0.40$  occurred only at one site, Kunming, and then only in fall and winter. Monthly average AODs  $> 0.60$  were found in central and eastern China all year around. The AODs in the Taklimakan desert region were  $> 0.60$  in spring and summer but  $< 0.60$  in fall and winter, and this pattern can be explained by the frequent dust storms in spring and summer and fewer dust events in fall and winter (Gong et al., 2003; Eck et al., 2005). It was also found that the AODs were  $< 0.40$  at the sites near the boundary between China and Mongolia, and this was true throughout the year. There also were more sites with low AODs, that is  $< 0.20$ , in fall (6 sites) and winter (9 sites) compared with spring (2 sites) and summer (3 sites).

## Ground-based aerosol climatology of China

H. Che et al.

[Title Page](#)[Abstract](#)[Introduction](#)[Conclusions](#)[References](#)[Tables](#)[Figures](#)[Back](#)[Close](#)[Full Screen / Esc](#)[Printer-friendly Version](#)[Interactive Discussion](#)

## Ground-based aerosol climatology of China

H. Che et al.

Title Page

Abstract

Introduction

Conclusions

References

Tables

Figures



Back

Close

Full Screen / Esc

Printer-friendly Version

Interactive Discussion



The spatial distributions of Alpha for the four seasons are presented in Fig. 3f–i. Eck et al. (2005) suggested that coarse mode aerosols were relatively more abundant when Alpha was less than 0.80. In this study, there were 24, 10, 14, and 15 sites with Alpha < 0.60 in spring, summer, fall, and winter season, respectively, and almost all of these sites are located in north China. This reflects the presence of coarse dust particles transported from semi-arid and arid regions of northwestern and northern China. Alpha > 0.80 were found in central and east China from summer to winter and in south China all year around, suggesting that the particle size distributions favored the fine mode.

In spring, there were many sites with Alpha 0.80–1.00 in central China and 1.00–1.20 in the Yangtze River delta region, and these values were obviously lower than in the other seasons when they were typically > 1.20. These results reflect the transport of large dust particles from northwest China to eastern China during the spring (Chen et al., 2009). As for the Taklimakan desert region itself, Alphas were < 0.40 from spring to fall and 0.40–0.60 in winter, and this implies the presence of coarse mode aerosols throughout the year, with greater impacts of fine-particle pollution sources in winter (Che et al., 2013). For southern China, including the stations at Nanning and Panyu, Alpha was > 1.20 all year, and this reflects the dominance of fine mode particles caused by the chronic anthropogenic emissions in the region (Tan et al., 2009).

### 3.1.2 Aerosol optical properties in remote, rural, and urban regions of China

From Fig. 4a and b, one can see small AODs at the four remote sites of Akedala, Lhasa, Mt. Waliguan, and Shangri-La. Indeed, the AODs at these sites were 0.11–0.18, with an arithmetic mean of  $0.14 \pm 0.04$ . The Angstrom exponent varied from 0.59 at Mt. Waliguan to 1.29 at Shangri-La and averaged  $0.97 \pm 0.29$ . These results are generally representative of the aerosol optical properties at background regions in the interior of Asia. Che et al. (2011) reported that the AOD at 500 nm at Mt. Waliguan averaged  $\sim 0.14$  from September 2009 to August 2010, and this is similar to the long-

term measurements reported here (AOD =  $0.14 \pm 0.06$  at 440 nm and Angstrom exponent =  $0.59 \pm 0.21$  from March 2009–April 2012).

The AODs for eleven rural stations in desert regions varied from 0.23 to 0.61 and averaged  $0.34 \pm 0.12$ . Although some stations, such as Ejina, Jiuquan, Dunhuang, and Minqin, near desert regions are known to be frequently affected by springtime dust storms, the average AODs were not as large as one might expect. In fact, the AODs at most of these sites were  $< 0.40$  except for Tazhong (AOD =  $0.53 \pm 0.28$ ) and Hotan (AOD =  $0.61 \pm 0.22$ ). These two stations are located in Taklimakan desert region, one of the world's largest sources for desert dust (Zhang et al., 1997; Che et al., 2013). The Alphas over the rural desert stations varied from 0.22–0.80 and averaged  $0.55 \pm 0.19$ , and these values reflect the light extinction properties of coarse dust particles.

The four rural stations located on the Chinese Loess Plateau (CLP) showed ranges in the AODs and Alphas of 0.37–0.46 and 0.79–0.89, respectively, and means of  $0.42 \pm 0.05$  and  $0.82 \pm 0.05$ . These values are consistent with the results reported by Bi et al. (2011) who studied aerosol optical properties at SACOL rural site on the CLP and reported AODs and Alphas of  $\sim 0.35$  and  $\sim 0.92$  respectively. The average AODs and Alphas at the CLP stations,  $0.34 \pm 0.12$  for AOD and  $0.55 \pm 0.19$  for Alpha, were higher than those over the desert regions. This shows that the aerosol loadings over the Loess Plateau were greater compared with the desert regions and that there were relatively more fine particles. The numbers of persons living in and around the CLP sites are larger than those at the desert stations, and as a result more anthropogenic aerosols likely occurred over the CLP. In fact, earlier studies have shown that both anthropogenic emissions and dust storms do affect the aerosol populations of the CLP. (Alfaro et al., 2003; Che et al., 2009c).

The AODs at ten rural sites in central and eastern China show obviously higher AODs compared with stations located near the deserts or CLP. The average AOD and Alpha for the rural sites were  $0.54 \pm 0.18$  and  $1.19 \pm 0.12$ , respectively. The AODs also varied over a large range, from 0.26 to 0.78, and the Alphas at all these sites were  $> 1.00$  and varied from 1.2 to 1.38, suggesting a dominance of fine particles. The sites in eastern

## Ground-based aerosol climatology of China

H. Che et al.

Title Page

Abstract

Introduction

Conclusions

References

Tables

Figures



Back

Close

Full Screen / Esc

Printer-friendly Version

Interactive Discussion



China are strongly influenced by anthropogenic emissions because even though their populations are relatively small, the sites are downwind of mega-cities. For example, the sites at Shangdianzi and Gucheng are near Beijing while Dongtan and Lin'an are near Shanghai (Che et al., 2009b).

The AODs for the urban CARSNET sites showed a range 0.4–1.00 with an average  $0.74 \pm 0.18$  while Alpha ranged from 0.52–1.50 and averaged  $1.05 \pm 0.23$ . The large AOD and Alpha > 1.00 indicates the aerosol populations were predominantly composed of fine mode particles. However, the average Alpha for urban sites was lower than that of rural sites at eastern China, and this is probably due to the presence of fugitive dust. Chen et al. (2010), for instance, pointed out that fugitive dusts from transportation, building construction, and burning garbage are a major component of the aerosol in metropolitan areas of China.

Figure 5 shows the seasonal variations in AOD (a–d) and Alpha (e–h) at the CARSNET remote, rural, and urban sites. In general, the AODs were lower at all three types of sites in fall and winter compared with spring and summer. The combined AODs in spring and summer were factors of 1.57, 1.62, 1.29, 1.18, and 1.14 to combined AODs in fall and winter at remote, rural, and urban sites, respectively. However, the Alphas in fall and winter were factors of 1.27, 1.28, 1.11, 1.10, and 1.09 to spring and summer seasons. These comparisons show that the effects of dust particles on AOD and Alpha were more apparent at the remote and rural desert sites compared with the rural and urban sites.

## 3.2 Temporal variations in AOD and Alpha

### 3.2.1 Monthly average AODs and variations in Alpha at remote sites

The AODs at Akedala in northwest China showed high monthly means (> 0.20) from February to April, and this was presumably a consequence of the transport of mineral dust from the nearby Gobi, sandy lands, and deserts as well as the deserts in eastern Kazakhstan. The AODs were lower from August to October when there was more pre-

## Ground-based aerosol climatology of China

H. Che et al.

Title Page

Abstract

Introduction

Conclusions

References

Tables

Figures



Back

Close

Full Screen / Esc

Printer-friendly Version

Interactive Discussion



**Ground-based  
aerosol climatology  
of China**

H. Che et al.

Title Page

Abstract

Introduction

Conclusions

References

Tables

Figures



Back

Close

Full Screen / Esc

Printer-friendly Version

Interactive Discussion



5 precipitation in the region and the winds were weaker. The AOD at Akedala was  $> 0.20$  in June and July, and this can be attributed to the transport of pollutants from countries in eastern Europe, western Russia, and eastern Kazakhstan, which are all upwind (Qu et al., 2008). The AODs increased from October to December, and that was probably

10 The AODs in spring and summer were high and low in fall and winter at Lhasa and Mt. Waliguan, which are both on the Tibetan Plateau. Monthly average AODs at these two sites exceeded 0.15 in spring and 0.10 in summer, and they were  $< 0.10$  in fall and winter. The AODs reported here for Lhasa are slightly larger than those in a study  
15 by Cong et al. (2009), and this could be caused by year-to-year differences in the strengths and numbers of dust storms as well as local contributions from anthropogenic activities. The CARSNET Lhasa site is located in the city itself, while Nam Co station of AERONET is 125 km north to Lhasa city, where there are no impacts from local anthropogenic activities (Cong et al., 2009). The AODs at Mt. Waliguan ( $0.14 \pm 0.06$ )  
20 were slightly larger than those at Shangri-La or Lhasa where the mean AOD values were  $0.11 \pm 0.05$  and  $0.11 \pm 0.03$ , respectively. The AODs at Shangri-La in southwestern China also showed two seasonal peaks; that is, the AODs were  $> 0.10$  during March to May and again from July to September while in other periods, the AODs were  $< 0.10$ . These small AODs at Shangri-La also show that even the maximum aerosol loadings  
25 in this region are very low compared with other regions in China.

In general, the monthly average Alphas at Akedala and Shangri-La and were larger than those that at Mt. Waliguan and Lhasa, and this indicates that the aerosol particles tend to be smaller at the latter two sites. This is likely due to the fact that Mt. Waliguan is located on the northwestern margin of Qinghai-Tibet plateau and therefore subject  
30 to the transport of dust from desert regions in western China and middle Asia (Che et al., 2011; Gong et al., 2003). Lhasa also can be affected by mineral aerosol from deserts in western China and local dust uplifted from Tibetan Plateau. The monthly averages for Alpha at Akedala, Mt. Waliguan and Lhasa were lower in spring than other seasons: the minima at these three sites occurred in March, with values of  $0.90 \pm 0.68$ ,

0.25 ± 0.14, and 0.53 ± 0.12, respectively. These low springtime Alphas suggest that coarse particles from dust events were prevalent at these three sites. In summer and fall, the Alphas were larger than in spring, with a maximum of 0.96 ± 0.38 in July at Waliguan and 1.22 ± 0.35 in August at Lahsa. At Shangri-La and Akedala, the Alphas were > 0.80 throughout the year, and therefore, fine mode particles were relatively abundant at these two sites.

### 3.2.2 Variations in monthly AODs and Alphas at the rural desert sites

Most of the eleven rural CARSNET sites near the desert regions showed large AODs in spring and summer and low AODs in autumn and winter, and this is evidence that the aerosol populations at these sites were affected by springtime dust events. In summer, the impacts from dust events weakened while anthropogenic emissions from central and western China evidently contributed to the aerosol loadings over these regions (Che et al., 2009c). In autumn and winter, dust storms are rare because low temperatures restrict convection even though incursions of cold air can bring strong winds. Hotan and Tazhong, the two rural sites located in Taklimakan desert, showed AOD > 0.40 from February to October. The monthly-averaged AODs were the lowest in November, 0.31 ± 0.12 at Hotan and 0.22 ± 0.16 at Tazhong. The four rural sites in desert regions of northwestern China each showed maximum AODs in April; these were 0.39 ± 0.30 at Ejina, 0.48 ± 0.27 at Minqin, 0.55 ± 0.41 at Dunhuang, and 0.55 ± 0.40 at Juquan. The minima occurred in fall or winter, with values of 0.14 ± 0.08, 0.20 ± 0.09, 0.17 ± 0.04 in November at Ejina, Dunhuang, Jiuquan, respectively, and 0.26 ± 0.18 in January at Minqin.

The four rural sites in the interior of Inner Mongolia showed generally similar variations in the AODs; that is, maxima in June of 0.44 ± 0.39, 0.39 ± 0.30, 0.49 ± 0.43, 0.45 ± 0.26 at Wulate, Xilinhot, Zhurihe, and Zhangbei, respectively. Minima in the AODs occurred in November at Ulate and Xilinhot with averages of 0.19 ± 0.09 and 0.16 ± 0.09, respectively, while the minima at Zhurihe (0.11 ± 0.05) and Zhangbei (0.18 ± 0.12) were in January. The low AODs in winter and autumn occurred when the ground surface

was often frozen or covered by snow – conditions that would prevent the production of windblown dust.

Monthly average Alphas at most of the rural desert sites, including Ejina, Zhangbei, Jiuquan, Dunhuang, Tazhong and Hotan, showed low values ( $< 0.80$ ) all year; and this indicates the coarse particles were the dominant aerosol components. As for other sites (Zhurihe, Hami, Xilinhot, Wulate, and Minqin), the Alphas were  $< 0.80$  in March and April when dust events were common. The two sites in the Taklimakan showed low Alphas ( $< 0.20$ ) for more than six months (February to October), and therefore large dust particles affected these sites more than the others. In December and January, the Alphas at most of the CARSNET rural desert sites were higher compared with the other types of sites, and this was likely due to presence of fine particles from coal and biomass burning as both used extensively for domestic heating (Eck et al., 2005).

### 3.2.3 Variations in monthly average AODs and Alphas at the rural sites on the Loess Plateau

The monthly average AODs at the four sites on the Loess Plateau showed different temporal trends. At Dongsheng, the AOD was  $> 0.40$  in spring and summer, and the monthly maximum ( $0.71 \pm 0.44$ ) occurred in June; and that was probably caused by the hygroscopic growth of particles in combination with gas-particle conversion processes (Eck et al., 2005). At Yan'an, the AOD varied smoothly around 0.35 from January to October, and it was  $< 0.30$  in November and December. At Mt. Gaolan the AODs in spring and winter were higher than in summer and autumn while at Yulin, the AODs were  $> 0.30$  from January to September. The seasonal variability in the aerosol at Yulin was likely caused by a mixture of dust and local anthropogenic emissions (Alfaro et al., 2003).

The Alphas for the four sites on the CLP showed obvious seasonality, with Alpha  $< 0.70$  from March to May but higher values ( $\sim 0.85$ ) in August. This is another indication that aerosol particles at these sites are affected both by dust events and anthropogenic activities (Fig. 11).

Title Page

Abstract

Introduction

Conclusions

References

Tables

Figures



Back

Close

Full Screen / Esc

Printer-friendly Version

Interactive Discussion



### 3.2.4 Variations in the monthly average AODs and Alphas at rural sites in central and eastern China

The rural CARSNET sites in central and eastern China can be divided into three groups (1) Tongyu and Mt. Longfeng located in northeastern China, (2) Shangdianzi, Gucheng, Huimin, Yushe and Mt. Tai in the North China Plain; and (3) Changde, Lin'an, and Dongtan in the middle and lower reaches of the Yangtze River. The AODs at Mt. Longfeng and Tongyu in northeast China and Mt. Tai in north China were  $\sim 0.3$ , which is lower compared with the rural stations in central and eastern China (Fig. 12). The AODs at Shangdianzi – the background site for the Beijing–Tianjin–Hebei (Jing–Jin–Ji) region was a factor of 1.6 ( $\sim 0.48$ ) greater than at the three sites just discussed, indicating higher aerosol loadings in this region.

The AODs at Huimin, Gucheng and Yushe in the North China Plain ranged from 0.58–0.71 as a result of the heavy pollution aerosol loadings there. This region of north China is industrially developed, and biomass burning is also common, especially in June and from September to October (Eck et al., 2010). For Dongtan, Changde, and Lin'an, the sites in the Yangtze River region of southern China, the AODs were 0.59–0.78, and these were higher than in the North China Plain. Mt. Longfeng and Tongyu in northeastern China showed AODs  $> 0.35$  during April to June, and the springtime values were obviously higher compared with the other months.

In June, the AODs for the North China Plain and Yangtze River delta station (Shangdianzi, Mt. Tai, Gucheng, Huimin, Lin'an, Dongtan) were quite high, most likely as a result of the burning of the straw (Logan et al., 2013). Indeed, the AODs at Gucheng, a site surrounded by farmlands, were higher in September than in the prior month or the two following months; and this is likely because peasants typically burn straw from agricultural fields in September. Similarly, the AODs at Tongyu were as high as 0.34 in October, and this also may have been due to the burning of biomass in nearby farmlands.

Title Page

Abstract

Introduction

Conclusions

References

Tables

Figures



Back

Close

Full Screen / Esc

Printer-friendly Version

Interactive Discussion



**Ground-based  
aerosol climatology  
of China**

H. Che et al.

[Title Page](#)[Abstract](#)[Introduction](#)[Conclusions](#)[References](#)[Tables](#)[Figures](#)[Back](#)[Close](#)[Full Screen / Esc](#)[Printer-friendly Version](#)[Interactive Discussion](#)

Shangdianzi and Mt. Tai showed similar monthly variations in AODs: they increased from January (0.20–0.30) to June (0.60–0.70) and then decreased through December (0.20–0.30). Gucheng and Huimin are located near farmlands, and the changes in monthly average AOD were not as obvious as at Shangdianzi and Mt. Tai where there are fewer local anthropogenic activities (Hänel et al., 2012). Nevertheless, in general, the temporal variations were similar for the four sites on the North China Plain. The AOD at Yushe was  $< 0.40$  from October to December, probably due to the influx of cold air in fall and winter which flushes polluted air from region. The monthly variations at Lin'an, Dongtan, and Changde, in middle and lower Yangtze River region, were different from the rural sites of northern China. The AOD of Changde was  $> 0.70$  from January–March and in September but  $< 0.60$  in the other months, and this is consistent with what has been reported for other urban areas in the middle section of the Yangtze River (Gong et al., 2014). The AOD at Lin'an was  $< 0.70$  only in July and November–December; the maximum monthly average was  $0.96 \pm 0.32$  in June, and the minimum ( $0.58 \pm 0.34$ ) was in July. At Dongtan, the AODs were  $< 0.45$  from September to October and  $\sim 0.80$  in February and August.

In general, the Alphas at the rural sites in central and eastern China were relatively low from March to May compared with other months, and that reflects the influence of coarse particles. Alpha at Tongyu, Mt. Longfeng, Shangdianzi, Gucheng, Huimin, Lin'an, and Dongtan was  $> 0.90$  throughout the year. Three of these sites have monthly average Alphas  $> 0.80$  from summer through winter, but in spring they are  $< 0.80$  at Yushe (March and April), Changde (April), and Mt. Tai (April and May). Thus, we conclude that fine mode particles were relatively abundant at the rural sites in central and eastern China, and that was most likely due to anthropogenic emissions (e.g. coal combustion, biomass burning, gas-particle conversion). The high relative abundance of fine particles was notably different from the rural sites in other regions of China, including the nearby desert and CLP sites, where there were more coarse-mode particles.

From June to September, which is the biomass burning season at the rural sites of Tongyu, Shangdianzi, Mt. Tai, Gucheng, Huimin, Lin'an, and Dongtan, the Alpha





**Ground-based  
aerosol climatology  
of China**

H. Che et al.

Title Page

Abstract

Introduction

Conclusions

References

Tables

Figures



Back

Close

Full Screen / Esc

Printer-friendly Version

Interactive Discussion



cating a regional veil of pollution, and this result is in agreement with previous observations made by Wang et al. (2012) and Xiao et al. (2011). Monthly average AODs  $> 1.00$  were observed from June to August, and these values are about a factor of two higher than the minimum monthly AODs. Furthermore, the AODs in June were higher than those in May at each of the four sites, and the high loadings were likely caused by the burning of agricultural crop residues (Cheng et al., 2014). The AOD at Pudong was lower than that at Hefei, Nanjing, or Hangzhou: the monthly means at Pudong were  $\sim 0.70$  during September to January. These low values are more than likely because Pudong is located near the coast, and polluted air can be replaced by cleaner air from the East Sea (Pan et al., 2010).

Panyu and Nanning, two urban sites in southern China, show temporal patterns different from the Yangtze River delta sites. AODs were high ( $> 0.80$ ) at the two sites during two periods, first from March to April and second from September to October, and during both of these periods, biomass burning is frequent with high relative humidity (Andreae et al., 2008; Tan et al., 2009). Interestingly, the AODs were low, from 0.46–0.66, in June and July at both sites, and these were roughly half of the monthly maximum AODs, which were found in March with  $\sim 1.20$  for both sites. This could be due to relative abundance of rain in the late spring and early summer and the resulting removal of PM by wet deposition as well as changes in emissions (Tan et al., 2009).

The variations in AODs at Chengdu and Kunming, two urban sites in southwestern China, differed from each other. The AODs at Chengdu were  $> 0.50$  throughout the year and  $> 1.00$  from December to April, with a maximum monthly mean of  $1.30 \pm 0.40$  in March. Clearly, the aerosol loadings at Chengdu were very heavy, and this is consistent with previous measurements. Indeed, high aerosol loadings in the Sichuan Basin have been attributed to unremitting anthropogenic emissions coupled with the physical trapping of pollutants in the basin (Luo et al., 2001; Li et al., 2003; Liu et al., 2014). In comparison, the AODs at Kunming were low ( $< 0.30$ ) from October to February, which is the dry season. High AODs ( $> 0.40$ ) at Kunming were found from March to September, which are in the wet season when the hygroscopic growth of the particles would

be expected. The AODs at both Chengdu and Kunming were high in March and August compared with other periods, probably due to the effects of seasonal biomass burning.

Except for Nanning and Kunming in southern China, almost all of the urban sites showed lower Angstrom exponents from March to May compared with other periods, but the patterns varied somewhat among sites (Fig. 15). At the urban sites in northwest, north, and northeast China (except for Dalian and Tianjin – two coastal sites), Alphas were  $< 0.80$  from March to April, but again there were some variations among sites. In contrast, the Alphas for the sites in southern China were generally  $> 0.80$  during this period even though they were lower than in other months. This pattern is evidence that coarse particles, especially mineral dust, have a greater effect on the northern urban sites than the southern ones.

These coarse particles include not only natural dust transported from the deserts in north and northwest China but also fugitive dusts. Indeed, large quantities of fugitive dust have been produced in some urban areas as a result of increased vehicular traffic and a boom in building construction (Fan et al., 2009). Preparations of agricultural fields for the planting of crops also cause the emission of mineral aerosol in spring, and this material can be transported to urban areas (Mei et al., 2004). From June to August, a great majority of the Alphas were  $> 1.00$ , indicating that fine mode aerosols were dominant at this time of year. Many of these fine particles were likely produced by gas-particle conversion reactions, and numerous studies which have shown that the volatile organic compounds are converted into secondary organic aerosols in summer as a result of conditions favorable for photochemical reactions (Shao et al., 2009). The high humidity in summer also leads to the hygroscopic growth of fine PM (Eck et al., 2010), and these processes undoubtedly affected the Alphas at some of the urban CARSNET sites.

The effects of biomass burning on the Alpha values for the urban CARSNET sites are not as apparent as at the rural sites in central and eastern China. Nevertheless, at some of urban sites, including Beijing, Hefei, Nanjing, Pudong, Hangzhou, and Panyu, the Alphas were high in June and from September to October, and this may be related

---

## Ground-based aerosol climatology of China

H. Che et al.

---

[Title Page](#)[Abstract](#)[Introduction](#)[Conclusions](#)[References](#)[Tables](#)[Figures](#)[Back](#)[Close](#)[Full Screen / Esc](#)[Printer-friendly Version](#)[Interactive Discussion](#)

to the emissions of fine particles from biomass burning. However, because the aerosol sources in these urban sites are complex and not well understood, more studies are needed to investigate this possibility.

### 3.3 Comparisons of urban stations with rural stations

5 Rapid urbanization in parts of China has perturbed the atmosphere and caused a variety of problems, including visibility impairment and air pollution, etc. (Che et al., 2007). CARSNET operates two pairs of sites with both urban sites and rural stations. From Figs. 12 and 14, one can see that both the AODs and the Alphas at Beijing and its paired rural site Shangdianzi showed very consistent temporal variations although the  
10 AOD at Shangdianzi was of course, much lower than that at Beijing. The Alpha at Beijing was lower than that at Shangdianzi, which shows that the particles in the urban area were larger than those at the rural site. This can be explained by the greater production of fugitive dusts in the urban region (Fan et al., 2009) and the settling out of larger particles during transport to the rural site. Transportation, construction activities, bare surfaces all cause the emission of fugitive dust particles in Beijing and other large cities  
15 (Chen et al., 2010). On the other hand, the surfaces at Shangdianzi are more heavily vegetated, and this tends to suppress the production of PM in the area.

The AODs and Alphas at the urban Lanzhou site were both higher than at the rural site at Mt. Gaolan (Figs. 14 and 10), which is about 600 m higher than the urban site – this was true throughout the year. The AODs at Lanzhou varied in the same way as  
20 at Mt. Gaolan from April to September, but they differed from October to April, and this decoupling probably results from changes in the surface boundary layer. From April to September, the boundary layer at both sites is normally deep, and this promotes similar variations in the aerosol populations at the two sites. From September to April,  
25 however, convection tends to be weak and the boundary layer at Lanzhou is lower than at Mt. Gaolan. The aerosol particles are then mainly concentrated in the shallower boundary layer, and that is why the AODs at the two sites become uncoupled from September to April.

## Ground-based aerosol climatology of China

H. Che et al.

Title Page

Abstract

Introduction

Conclusions

References

Tables

Figures



Back

Close

Full Screen / Esc

Printer-friendly Version

Interactive Discussion



**Ground-based  
aerosol climatology  
of China**

H. Che et al.

[Title Page](#)[Abstract](#)[Introduction](#)[Conclusions](#)[References](#)[Tables](#)[Figures](#)[Back](#)[Close](#)[Full Screen / Esc](#)[Printer-friendly Version](#)[Interactive Discussion](#)

In contrast to the AODs, the Alpha values varied coherently at Lanzhou and Mt. Gaolan (Figs. 15 and 11), and this is likely because this parameter is not concentration dependent. That is, the aerosol size variations at both sites are similar throughout the year even though the Alpha at Lanzhou was  $> 1.00$  and  $< 1.00$  at Mt. Gaolan. The Alpha values show that while the particles were mainly fine mode at both sites, they were even smaller at Lanzhou, and this difference in particle size can be explained by types of sources for the PM. Mt. Gaolan is located on the CLP where there is little vegetative cover, and large dust particles can be raised from local and regional sources. In Lanzhou, there is an abundance of anthropogenic sources for fine particles, and the production of secondary aerosol particles also contributes to fine PM and Alphas  $> 1.00$  (Wang et al., 2010).

### 3.4 Long-term variations of AODs over China

The variations in annual AODs for the twelve CARSNET sites that were in operation for the entire study period, that is from 2002 to 2013, are shown in Fig. 16. These include five urban sites (Urumqi, Lanzhou, Beijing, Tianjin, and Datong), four rural desert sites (Tazhong, Ejina, Dunhuang, and Xilinhot), and three regional background sites (Mt. Longfeng, Shangdianzi, and Lin'an), and as a group, they can be considered a reasonable representation of how conditions have changed in China. As shown in Fig. 16, most of these sites showed overall decreases in AODs from 2006 to 2011; the one exception was Tazhong, which is in the central of the Taklimakan Desert. The decrease was not continuous, however as the AODs apparently increased from 2012 at some sites, including Urumqi, Ejina, Dunhuang, Tianjin, Beijing, Mt. Longfeng, and Shangdianzi.

The composited average AODs for these twelve sites was highest in 2003, and there was a slight decrease from 2006 to 2009 followed by an increase from 2009 to 2013 (Fig. 17a). From Fig. 17b, which shows the departure of the AODs from the average, we can see that AODs in 2003, 2006, and 2012 were 0.03–0.08 larger than the 12 yr average. Moreover, the composite AOD increased  $\sim 0.03$  from 2009 to 2013, and this



## 4 Summary and conclusions

In this study, data collected from the CARSNET network from 2002 to 2013 were used to characterize the aerosol optical properties over a large area of China. The AODs generally increased from north to south, and very low AODs ( $< 0.20$ ) were found only in remote regions, including the Tibetan Plateau and parts of northwestern China. Large AODs ( $> 0.60$ ) mainly occurred in central and eastern China where heavy industrial and other anthropogenic emissions led to high aerosol loadings. AOD levels of 0.20–0.40 were observed in semi-arid and arid regions as well as at some regional background areas in north and northeast China.

Large Alphas ( $> 1.20$ ), which are caused by large proportions of fine particles, were observed at the sites in the southern reaches of the Yangtze River and at the clean sites in northeastern China. In the desert regions of northwest China and industrial region of northeast China, the Alpha values were significantly lower ( $< 0.80$ ) compared with those in the central and eastern regions, such as the North China Plain, Guanzhong Plain, or Sichuan Basin.

For most sites in north China, the aerosol columnar extinctions were larger in spring and summer than in fall and winter. About half of the sites had Alpha  $< 0.60$  in spring, and this was due to large dust particles transported from semi-arid and arid regions in northwest and north China. Alpha  $> 0.80$  also occurred in central and east China region from summer to winter and in south China all year round, suggesting that fine-mode particles were the main components of the aerosol populations in those areas.

The AODs at the remote sites ranged from 0.11 to 0.18, and averaged  $0.14 \pm 0.04$  while the Angstrom exponents at those sites varied from 0.59–1.29 with an average of  $0.97 \pm 0.29$ . In comparison, the AODs at rural desert stations varied from 0.23 to 0.61 (average  $0.34 \pm 0.12$ ). The AODs and Alphas at the rural stations on the Loess Plateau were 0.37 to 0.46 and 0.79 to 0.89, respectively and the corresponding means were  $0.42 \pm 0.05$  and  $0.82 \pm 0.05$ . The AODs at rural sites in central and eastern China showed the much higher AODs compared with the rural sites close to deserts or located

Title Page

Abstract

Introduction

Conclusions

References

Tables

Figures



Back

Close

Full Screen / Esc

Printer-friendly Version

Interactive Discussion



**Ground-based  
aerosol climatology  
of China**

H. Che et al.

[Title Page](#)[Abstract](#)[Introduction](#)[Conclusions](#)[References](#)[Tables](#)[Figures](#)[Back](#)[Close](#)[Full Screen / Esc](#)[Printer-friendly Version](#)[Interactive Discussion](#)

on the CLP. The average AOD at rural sites of East China was  $0.54 \pm 0.18$  while the average Alpha was  $1.19 \pm 0.12$ . The AODs at this region varied over a large range, from 0.26 to 0.78, and the Alphas at all of these sites were larger than 1.00, ranging from 1.02 to 1.38, and suggesting the dominance of fine particles.

The monthly average AODs at the urban stations ranged from 0.40 to 1.00 with an average of  $0.74 \pm 0.18$ , and the range for the Alphas was 0.52–1.50 with average  $1.05 \pm 0.23$ ; these large Alphas indicate that the aerosols were predominately fine mode. The AODs were lower in remote, rural, and urban sites in fall and winter compared with spring and summer. However, the Alphas in fall and winter were larger than in the spring and summer seasons.

Monthly-averaged AODs and Alphas show different patterns at the remote, rural and urban sites, and this reflects the spatial and temporal heterogeneity of the aerosol. The most important factors driving the temporal variations in aerosol optical properties are the natural dust events and anthropogenic activities. In eastern China, the aerosol optical properties are affected by both natural and anthropogenic mineral dust from March to May, and burning of biomass and the formation of second aerosol particles contribute to the high AODs from June through October at most rural and urban sites. The aerosol optical properties in winter season are strongly affected by the burning of coal for heating, especially in north China.

A comparison of AODs and Alphas between pairs of urban and rural stations in Beijing and Lanzhou showed that seasonal variations in the vertical distribution of the aerosol cause changes significant in the aerosol optical properties. A comparison of the data for the Lanzhou–Mt. Gaolan paired sites indicated that the depth of the boundary was an important determinant of the seasonal variations of PM with height.

The annual variations in the AODs at the 12 CARSNET long-term (2002 to 2013) observation sites show a decreasing trend from 2006 to 2009 but an increase of  $\sim 0.03$  from 2009 to 2013. This suggests the possibility that the aerosol loadings in China have reversed a decreasing trend and increased in recent years. However, the year-to-year variability in AODs is affected by changes in the strength of the East Asian monsoon as

well as variations in emissions, and the interpretation of long-term records of aerosol optical properties needs to take both of these factors – and possibly others – into account.

Although this work is based on the longest and most extensive set of ground-based observations of aerosol optical properties made in China to date, it is just a first step towards understanding what controls the aerosol populations. More detailed work is needed in future, and we have developed a set of recommendations for continued monitoring efforts. First, CARSNET should continue collaborating with other international networks, including AERONET, PHOTONS, RIMA, SKYNET, etc. to ensure consistency in calibration protocols as well as cloud-screening and data retrieval processing procedures. Second, the network should be expanded and the studies extended in time to obtain more detailed information on the aerosol optical properties over China. Instrument and site maintenance should be top priorities as these efforts would improve data quality and minimize gaps in the data. Third, in addition to AOD and Alpha, other key parameters such as single scattering albedo, size distributions and the optical properties of fine mode particles should be measured. The results of our current project are potentially valuable for inter-comparisons with measurements made with satellites as well as for assimilation into and validation of aerosol models. Furthermore, the results are not only relevant for China but also for East Asia, and therefore, the data used to prepare the figures for this paper have been made available as Appendix tables.

*Acknowledgements.* This research was funded by the National Key Project of Basic Research (2011CB403401), the Project (41275167 and 41130104) supported by the National Natural Science Foundation of China, Strategic Priority Research Program of the Chinese Academy of Sciences (XDA05100301), and CAMS Basis Research Project (2014R17) and the Jiangsu Collaborative Innovation Center for Climate Change. The research leading to these results has received funding from the European Union Seventh Framework Programme (FP7/2007–2013) under grant agreement no. 262254.

Ground-based aerosol climatology of China

H. Che et al.

Title Page

Abstract Introduction

Conclusions References

Tables Figures

◀ ▶

◀ ▶

Back Close

Full Screen / Esc

Printer-friendly Version

Interactive Discussion



## References

- Alfaro, S. C., Gomes, L., Rajot, J. L., Lafon, S., Gaudichet, A., Chatenet, B., Maille, M., Cautenet, G., Lasserre, F., Cachier, H., and Zhang, X. Y.: Chemical and optical characterization of aerosols measured in spring 2002 at the ACE-Asia supersite, Zhenbeitai, China, *J. Geophys. Res.*, 108, 8641, doi:10.1029/2002JD003214, 2003.
- Andreae, M. O., Schmid, O., Yang, H., Chand, D., Yu, J., Zeng, L., and Zhang, Y.: Optical properties and chemical composition of the atmospheric aerosol in urban Guangzhou, China, *Atmos. Environ.*, 42, 6335–6350, 2008.
- Bi, J., Huang, J., Fu, Q., Wang, X., Shi, J., Zhang, W., Huang, Z., and Zhang, B.: Toward characterization of the aerosol optical properties over Loess Plateau of northwestern China, *J. Quant. Spectrosc. Ra.*, 112, 346–360, 2011.
- Bi, J., Huang, J., Fu, Q., Ge, J., Shi, J., Zhou, T., and Zhang, W.: Field measurement of clear-sky solar irradiance in Badain Jaran Desert of northwestern China *J. Quant. Spectrosc. Ra.*, 122, 194–207, 2013.
- Bokoye, A. I., Royer, A., O'Neill, N. T., Cliche, P., Fedosejevs, G., Teillet, P. M., and McArthur, L. J. B.: Characterization of atmospheric aerosols across Canada from a ground-based sunphotometer network: Aerocan, *Atmos. Ocean.*, 39, 429–456, 2001.
- Charlson, R. J., Schwartz, S. E., Hales, J. M., Cess, D., Coakley, J. A., and Hansen, J. E.: Climate forcing by anthropogenic aerosols, *Science*, 255, 423–430, 1992.
- Che, H. Z., Shi, G. Y., Zhang, X. Y., Arimoto, R., Zhao, J. Q., Xu, L., Wang, B., and Chen, Z. H.: Analysis of 40 years of solar radiation data from China, 1961–2000, *Geophys. Res. Lett.*, 32, L06803, doi:10.1029/2004GL022322, 2005.
- Che, H., Zhang, X., Li, Y., Zhou, Z., and Qu, J. J.: Horizontal visibility trends in China 1981–2005, *Geophys. Res. Lett.*, 34, L24706, doi:10.1029/2007GL031450, 2007.
- Che, H., Shi, G., Uchiyama, A., Yamazaki, A., Chen, H., Goloub, P., and Zhang, X.: Intercomparison between aerosol optical properties by a PREDE skyradiometer and CIMEL sunphotometer over Beijing, China, *Atmos. Chem. Phys.*, 8, 3199–3214, doi:10.5194/acp-8-3199-2008, 2008.
- Che, H., Zhang, X. Y., Chen, H. B., Damiri, B., Goloub, P., Li, Z. Q., Zhang, X. C., Wei, Y., Zhou, H. G., Dong, F., Li, D. P., and Zhou, T. M.: Instrument calibration and aerosol optical depth validation of the China Aerosol Remote Sensing Network, *J. Geophys. Res.*, 114, D03206, doi:10.1029/2008JD011030, 2009a.

**Ground-based  
aerosol climatology  
of China**

H. Che et al.

Title Page

Abstract

Introduction

Conclusions

References

Tables

Figures



Back

Close

Full Screen / Esc

Printer-friendly Version

Interactive Discussion



- Che, H., Yang, Z., Zhang, X., Zhu, C., Ma, Q., Zhou, H., and Wang, P.: Study on the aerosol optical properties and their relationship with aerosol chemical compositions over three regional background stations in China, *Atmos. Environ.*, 43, 1093–1099, doi:10.1016/j.atmosenv.2008.11.010, 2009b.
- 5 Che, H. Z., Zhang, X. Y., Alfraro, S., Chatenet, B., Gomes, L., and Zhao, J. Q.: Aerosol optical properties and its radiative forcing over Yulin, China in 2001 and 2002, *Adv. Atmos. Sci.*, 26, 564–576, doi:10.1007/s00376-009-0564-4, 2009c.
- Che, H., Wang, Y., and Sun, J.: Aerosol optical properties at Mt. Waliguan observatory, China, *Atmos. Environ.*, 45, 6004–6009, 2011.
- 10 Che, H., Wang, Y., Sun, J., Zhang, X., Zhang, X., and Guo, J.: Variation of aerosol optical properties over the Taklimakan Desert in China, *Aerosol Air Qual. Res.*, 13, 777–785, 2013.
- Che, H., Xia, X., Zhu, J., Li, Z., Dubovik, O., Holben, B., Goloub, P., Chen, H., Estelles, V., Cuevas-Agulló, E., Blarel, L., Wang, H., Zhao, H., Zhang, X., Wang, Y., Sun, J., Tao, R., Zhang, X., and Shi, G.: Column aerosol optical properties and aerosol radiative forcing during a serious haze-fog month over North China Plain in 2013 based on ground-based sun-  
15 photometer measurements, *Atmos. Chem. Phys.*, 14, 2125–2138, doi:10.5194/acp-14-2125-2014, 2014.
- Chen, D., Cheng, S., Zhou, Y., Guo, X., Fan, S., and Wang, H.: Impact of road fugitive dust on air quality in Beijing, China, *Environ. Eng. Sci.*, 27, 825–834, doi:10.1089/ees.2009.0122, 2010.
- 20 Chen, R., Li, Y., Ma, Y., Pan, G., Zeng, G., Xu, X., Chen, B., and Kan, H.: Coarse particles and mortality in three Chinese cities: the China Air Pollution and Health Effects Study (CAPES), *Sci. Total Environ.*, 409, 4934–4938, 2011.
- Chen, W., Chen, Y., Chou, C. K., Chang, S., Lin, P., and Chen, J.: Columnar optical properties of tropospheric aerosol by combined lidar and sunphotometer measurements at Taipei, Taiwan, *Atmos. Environ.*, 43, 2700–2708, 2009.
- 25 Cheng, Z., Wang, S., Fu, X., Watson, J. G., Jiang, J., Fu, Q., Chen, C., Xu, B., Yu, J., Chow, J. C., and Hao, J.: Impact of biomass burning on haze pollution in the Yangtze River delta, China: a case study in summer 2011, *Atmos. Chem. Phys.*, 14, 4573–4585, doi:10.5194/acp-14-4573-2014, 2014.
- 30 Chin, M.: Atmospheric science: dirtier air from a weaker monsoon, *Nat. Geosci.*, 5, 449–450, 2012.

**Ground-based  
aerosol climatology  
of China**

H. Che et al.

[Title Page](#)[Abstract](#)[Introduction](#)[Conclusions](#)[References](#)[Tables](#)[Figures](#)[Back](#)[Close](#)[Full Screen / Esc](#)[Printer-friendly Version](#)[Interactive Discussion](#)

Cong, Z. Y., Kang, S. C., Smirnov, A., and Holben, B.: Aerosol optical properties at Nam Co, a remote site in central Tibetan Plateau, *Atmos. Res.*, 92, 42–48, doi:10.1016/j.atmosenv.2010.04.013, 2009.

Dubovik, O. and King, M. D.: A flexible inversion algorithm for the retrieval of aerosol optical properties from Sun and sky radiance measurements, *J. Geophys. Res.*, 105, 20673–20696, doi:10.1029/2000JD900282, 2000a.

Dubovik, O., Smirnov, A., Holben, B. N., King, M. D., Kaufman, Y. J., Eck, T. F., and Slutsker, I.: Accuracy assessments of aerosol optical properties retrieved from Aerosol Robotic Network (AERONET) Sun and sky radiance measurements, *J. Geophys. Res.-Atmos.*, 105, 9791–9806, 2000b.

Eck, T. F., Holben, B. N., Reid, J. S., Dubovik, O., Smirnov, A., O'Neill, N. T., Slutsker, I., and Kinne, S.: Wavelength dependence of the optical depth of biomass burning, urban, and desert dust aerosols, *J. Geophys. Res.*, 104, 31333–31349, 1999.

Eck, T. F., Holben, B. N., Dubovik, O., Smirnov, A., Goloub, P., Chen, H. B., Chatenet, B., Gomes, L., Zhang, X. Y., Tsay, S. C., Ji, Q., Giles, D., and Slutsker, I.: Columnar aerosol optical properties at AERONET sites in central eastern Asia and aerosol transport to the tropical mid-Pacific, *J. Geophys. Res.*, 110, D06202, doi:10.1029/2004JD005274, 2005.

Eck, T. F., Holben, B. N., Sinyuk, A., Pinker, R. T., Goloub, P., Chen, H., Chatenet, B., Li, Z., Singh, R. P., Tripathi, S. N., Reid, J. S., Giles, D. M., Dubovik, O., O'Neill, N. T., Smirnov, A., Wang, P., and Xia, X.: Climatological aspects of the optical properties of fine/coarse mode aerosol mixtures, *J. Geophys. Res.*, 115, D19205, doi:10.1029/2010JD014002, 2010.

Fan, S., Tian, G., Li, G., Huang, Y., Qin, J., and Cheng, S.: Road fugitive dust emission characteristics in Beijing during Olympics Game 2008 in Beijing, China, *Atmos. Environ.*, 43, 6003–6010, 2009.

Fan, X., Chen, H., Goloub, P., Xia, X., Zhang, W., and Chatenet, B.: Analysis of column-integrated aerosol optical thickness in Beijing from AERONET observations, *China Part.*, 4, 330–335, 2006.

Fan, X. H., Xia, X. A., and Chen, H. B.: Comparison of column-integrated aerosol optical and physical properties in an urban and suburban site on the North China Plain, *Adv. Atmos. Sci.*, 32, 477–486, doi:10.1007/s00376-014-4097-0, 2015.

Fu, G., Yu, J., Zhang, Y., and Hu, S.: Temporal variation of wind speed in China for 1961–2007, *Theor. Appl. Climatol.*, 104, 313–324, 2011.

## Ground-based aerosol climatology of China

H. Che et al.

Title Page

Abstract

Introduction

Conclusions

References

Tables

Figures



Back

Close

Full Screen / Esc

Printer-friendly Version

Interactive Discussion



- Goloub, P., Li, Z., Dubovik, O., Blarel, L., Podvin, T., Jankowiak, I., Lecoq, R., Deroo, C., Chatenet, B., Morel, J. P., Cuevas, E., and Ramos, R.: PHOTONS/AERONET sun-photometer network overview: description, activities, results, P. SPIE, 6936, 69360V, doi:10.1117/12.783171, 2007.
- 5 Gong, S. L., Zhang, X. Y., Zhao, T. L., McKendry, I. G., Jaffe, D. A., and Lu, N. M.: Characterization of soil dust aerosol in China and its transport and distribution during 2001 ACE-Asia: 2. Model simulation and validation, J. Geophys. Res., 108, 4262, doi:10.1029/2002JD002633, 2003.
- Gong, W., Zhang, S., and Ma, Y.: Aerosol optical properties and determination of aerosol size distribution in Wuhan, China, Atmosphere, 5, 81–91, doi:10.3390/atmos5010081, 2014.
- 10 Hansen, J., Sato, M., and Ruedy, R.: Radiative forcing and climate response, J. Geophys. Res., 102, 6831–6864, doi:10.1029/96JD03436, 1997.
- Hansen, J., Sato, M., Ruedy, R., Lacis, A., and Oinas, V.: Global warming in the twenty-first century: an alternative scenario, P. Natl. Acad. Sci. USA, 97, 9875–9880, 2000.
- 15 Hänel, A., Baars, H., Althausen, D., Ansmann, A., Engelmann, R., and Sun, J. Y.: One-year aerosol profiling with EUCAARI Raman lidar at Shangdianzi GAW station: Beijing plume and seasonal variations, J. Geophys. Res., 117, D13201, doi:10.1029/2012JD017577, 2012.
- Holben, B., Tanre, D., Smirnov, A., Eck, T., Slutsker, I., Abuhassan, N., Newcomb, W. W., Schafer, J., Chatenet, B., Lavenue, F., Kaufman, Y., Castle, J. V., Setzer, A., Markham, B., Clark, D., Frouin, R., Halthore, R., Karnieli, A., O'Neill, N., Pietras, C., Pinker, R., Voss, K., and Zibordi, G.: An emerging ground-based aerosol climatology: aerosol optical depth from AERONET, J. Geophys. Res., 106, 12067–12097, 2001.
- 20 Holben, B. N., Eck, T. F., Slutsker, I., Tanre, D., Buis, J. P., Setzer, A., Vermote, E., Reagan, J. A., Kaufman, Y., Nakajima, T., Lavenu, F., Jankowiak, I., and Smirnov, A.: AERONET – a federated instrument network and data archive for aerosol characterization, Remote Sens. Environ., 66, 1–16, 1998.
- 25 Hu, X., Zhang, Y., Zhang, G., Huang, Y., and Wang, Y.: Measurements and study of aerosol optical characteristics in China radiometric calibration site, J. Appl. Meteorol. Sci., 12, 257–266, 2001 (in Chinese).
- 30 Huebert, B. J., Bates, T., Russell, P. B., Shi, G., Kim, Y. J., Kawamura, K., Carmichael, G., and Nakajima, T.: An overview of ACE-Asia: strategies for quantifying the relationships between Asian aerosols and their climatic impacts, J. Geophys. Res., 108, 8633, doi:10.1029/2003JD003550, 2003.

## Ground-based aerosol climatology of China

H. Che et al.

Title Page

Abstract

Introduction

Conclusions

References

Tables

Figures



Back

Close

Full Screen / Esc

Printer-friendly Version

Interactive Discussion



- IPCC: Climate Change 2007: The Scientific Basis, Forth Assessment Report, Cambridge University Press, New York, 2007.
- IPCC: Climate Change 2013: The Physical Science Basis. Contribution of Working Group I to the Fifth Assessment Report of the Intergovernmental Panel on Climate Change, edited by: Stocker, T. F., Qin, D., Plattner, G.-K., Tignor, M., Allen, S. K., Boschung, J., Nauels, A., Xia, Y., Bex, V., and Midgley, P. M., Cambridge, UK and New York, 2013.
- Jiang, Y., Luo, Y., Zhao, Z., and Tao, S.: Changes in wind speed over China during 1956–2004, *Theor. Appl. Climatol.*, 99, 421–430, 2010.
- Kim, D. H., Sohn, B. J., Nakajima, T., Takamura, T., Takemura, T., Choi, B. C., and Yoon, S. C.: Aerosol optical properties over east Asia determined from ground-based sky radiation measurements, *J. Geophys. Res.*, 109, D02209, doi:10.1029/2003JD003387, 2004.
- Kim, D. H., Sohn, B. J., Nakajima, T., and Takamura, T.: Aerosol radiative forcing over east Asia determined from ground-based solar radiation measurements, *J. Geophys. Res.*, 110, D10S22, doi:10.1029/2004JD004678, 2005.
- Lee, K., Li, Z., Cribb, M. C., Liu, J., Wang, L., Zheng, Y., Xia, X., Chen, H., and Li, B.: Aerosol optical depth measurements in eastern China and a new calibration method, *J. Geophys. Res.*, 115, D00K11, doi:10.1029/2009JD012812, 2010.
- Lei, Y., Zhang, Q., He, K. B., and Streets, D. G.: Primary anthropogenic aerosol emission trends for China, 1990–2005, *Atmos. Chem. Phys.*, 11, 931–954, doi:10.5194/acp-11-931-2011, 2011.
- Li, C. C., Mao, J. T., and Lau, K. H.: Characteristics of the aerosol optical depth distributions over Sichuan Basin derived from MODIS data, *J. Appl. Meteorol.*, 14, 1–7, 2003 (in Chinese).
- Li, F. and Lu, D.: Optical properties of atmospheric aerosols over Mount Qomolangma, *Chinese J. Atmos. Sci.*, 19, 755–763, 1995 (in Chinese).
- Li, X., Chen, Y., Hu, X., Ren, Y., and Wei, W.: Analysis of atmospheric aerosol properties over Urumqi, *China Environ. Sci.*, 25, 22–25, 2005 (in Chinese).
- Li, Z. Q., Xia, X. G., Cribb, M., Mi, W., Holben, B., Wang, P., Chen, H. B., Tsay, S. C., Eck, T. F., Zhao, F. S., Dutton, E. G., and Dickerson, R. E.: Aerosol optical properties and their radiative effects in northern China, *J. Geophys. Res.*, 112, D22S01, doi:10.1029/2006JD007382, 2007.
- Liang, F. and Xia, X. A.: Long-term trends in solar radiation and the associated climatic factors over China for 1961–2000, *Ann. Geophys.*, 23, 2425–2432, doi:10.5194/angeo-23-2425-2005, 2005.

**Ground-based  
aerosol climatology  
of China**

H. Che et al.

Title Page

Abstract

Introduction

Conclusions

References

Tables

Figures



Back

Close

Full Screen / Esc

Printer-friendly Version

Interactive Discussion



Lin, J., van Donkelaar, A., Xin, J., Che, H., and Wang, Y.: Clear-sky aerosol optical depth over east China estimated from visibility measurements and chemical transport modeling, *Atmos. Environ.*, 258–267, doi:10.1016/j.atmosenv.2014.06.044, 2014.

Liu, R., Li, L., Yu, J., Huang, W., Xu, L., Liu, M., and Tang, X.: On-line measurements and characteristic analysis of aerosol optical depth in the atmosphere of Urban Chongqing, *Acta Scientiae Circumstantiae*, 34, 819–825, 2014 (in Chinese).

Liu, X., Yan, L., Yang, P., Yin, Z., and North, G., R.: Influence of indian summer monsoon on aerosol loading in East Asia, *J. Appl. Meteorol. Clim.*, 50, 523–533, doi:10.1175/2010JAMC2414.1, 2011.

Liu, Y., Niu, S., and Zheng, Y.: Optical depth characteristics of Yinchuan atmospheric aerosols based on the CE-318 sun tracking spectrophotometer data, *J. Nanjing Inst. Meteor.*, 27, 615–632, 2004 (in Chinese).

Liu, Y., Huang, J., Shi, G., Takamura, T., Khatri, P., Bi, J., Shi, J., Wang, T., Wang, X., and Zhang, B.: Aerosol optical properties and radiative effect determined from sky-radiometer over Loess Plateau of Northwest China, *Atmos. Chem. Phys.*, 11, 11455–11463, doi:10.5194/acp-11-11455-2011, 2011.

Logan, T., Xi, B., Dong, X., Li, Z., and Cribb, M.: Classification and investigation of Asian aerosol absorptive properties, *Atmos. Chem. Phys.*, 13, 2253–2265, doi:10.5194/acp-13-2253-2013, 2013.

Luo, Y., Lu, D., Zhou, X., Li, W., and He, Q.: Characteristics of the spatial distribution and yearly variation of aerosol optical depth over China in last 30 years, *J. Geophys. Res.*, 106, 14501–14513, 2001.

Mao, J., Wang, Q., and Zhao, B.: The observation of the atmospheric transparency spectrum and the turbidity, *Acta Meteorol. Sin.*, 41, 322–331, 1983 (in Chinese).

Mei, F., Zhang, X., Lu, H., Shen, Z., and Wang, Y.: Characterization of MASDs of surface soils in north China and its influence on estimating dust emission, *Chin. Sci. Bull.*, 49, 2169–2176, 2004.

Mi, W., Li, Z., and Xia, X., Holben, B., Levy, R., Zhao, F., Chen, H., and Cribb, M.: Evaluation of the Moderate Resolution Imaging Spectroradiometer aerosol products at two Aerosol Robotic Network stations in China, *J. Geophys. Res.*, 112, D22S08, doi:10.1029/2007JD008474, 2007.

**Ground-based  
aerosol climatology  
of China**

H. Che et al.

Title Page

Abstract

Introduction

Conclusions

References

Tables

Figures



Back

Close

Full Screen / Esc

Printer-friendly Version

Interactive Discussion



- Pan, L., Che, H., Geng, F., Xia, X., Wang, Y., Zhu, C., Chen, M., Gao, W., and Guo, J.: Aerosol optical properties based on ground measurements over the Chinese Yangtze Delta region, *Atmos. Environ.*, 44, 2587–2596, 2010.
- Prats, N., Cachorro, V. E., Berjón, A., Toledano, C., and De Frutos, A. M.: Column-integrated aerosol microphysical properties from AERONET Sun photometer over southwestern Spain, *Atmos. Chem. Phys.*, 11, 12535–12547, doi:10.5194/acp-11-12535-2011, 2011.
- Qi, B., Du, R., Yu, Z., and Zhou, B.: Aerosol optical depth in urban site of Hangzhou, China *Environ. Sci.*, 34, 588–595, 2014 (in Chinese).
- Qin, S., Shi, G., Chen, L., Wang, B., Zhao, J., Yu, C., and Yang, S.: Long-term variation of aerosol optical depth in China based on meteorological horizontal visibility observations, *Chinese J. Atmos. Sci.*, 34, 449–456, doi:10.3878/j.issn.1006-9895.2010.02.18, 2010 (in Chinese).
- Qiu, J.: A method to determine atmospheric aerosol optical depth using total direct solar radiation, *J. Atmos. Sci.*, 55, 744–757, 1998.
- Qiu, J. and Yang, L.: Variation characteristics of atmospheric aerosol optical depths and visibility in North China during 1980–1994, *Atmos. Environ.*, 34, 603–609, 2000.
- Qiu, J. and Zhou, X.: Simultaneous determination of aerosol size distribution and refractive index and surface albedo from radiance – part I: Theory, *Adv. Atmos. Sci.*, 3, 162–171, 1986.
- Qiu, J., Wang, H., Zhou, X., and Lu, D.: Experimental study of remote sensing of atmospheric aerosol size distribution by combined solar extinction and forward scattering method, *Acta Meteorol. Sin.*, 7, 33–41, 1983.
- Qu, W., Zhang, Y., Arimoto, R., Wang, D., Wang, Y., Yan, Y., and Li, Y.: Chemical composition of the background aerosol at two sites in southwestern and northwestern China: potential influences of regional transport, *Tellus B*, 60, 657–673, 2008.
- Quan, X., Zhang, L., Cao, X., and Wang, H.: Property of aerosol optical depth over Lanzhou City in the winter of 2007, *J. Lanzhou Univ. Nat. Sci.*, 45, 39–44, 2009 (in Chinese).
- Ramanathan, V., Crutzen, P. J., Lelieveld, J., Mitra, A. P., Althausen, D., Anderson, J., Andreae, M. O., Cantrell, W., Cass, G. R., Chung, C. E., Clarke, A. D., Coakley, J. A., Collins, W. D., Conant, W. C., Dulac, F., Heintzenberg, J., Heymsfield, A. J., Holben, B., Howell, S., Hudson, J., Jayaraman, A., Kiehl, J. T., Krishnamurti, T. N., Lubin, D., McFarquhar, G., Novakov, T., Ogren, J. A., Podgorny, I. A., Prather, K., Priestley, K., Prospero, J. M., Quinn, P. K., Rajeev, K., Rasch, P., Rupert, S., Sadourny, R., Satheesh, S. K., Shaw, G. E.,

## Ground-based aerosol climatology of China

H. Che et al.

Title Page

Abstract

Introduction

Conclusions

References

Tables

Figures



Back

Close

Full Screen / Esc

Printer-friendly Version

Interactive Discussion



Sheridan, P., and Valero, F. P. J.: Indian Ocean Experiment: an integrated analysis of the climate forcing and effects of the great Indo–Asian haze, *J. Geophys. Res.*, 106, 28371–28398, 2001.

Seinfeld, J. H., Carmichael, G. R., Arimoto, R., Conant, W. C., Brechtel, F. J., Bates, T. S., Cahill, T. A., Clarke, A. D., Doherty, S. J., Flatau, P. J., Huebert, B. J., Kim, J., Markowicz, K. M., Quinn, P. K., Russell, L. M., Russell, P. B., Shimizu, A., Shinozuka, Y., Song, C. H., Tang, Y. H., Uno, I., Vogelmann, A. M., Weber, R. J., Woo, J. H., and Zhang, X. Y.: ACE-ASIA: regional climatic and atmospheric chemical effects of Asian dust and pollution, *B. Am. Meteorol. Soc.*, 85, 367–380, 2004.

Shao, M., Lu, S., Liu, Y., Xie, X., Chang, C., Huang, S., and Chen, Z.: Volatile organic compounds measured in summer in Beijing and their role in ground-level ozone formation, *J. Geophys. Res.*, 114, D00G06, doi:10.1029/2008JD010863, 2009.

Smirnov, A., Holben, B. N., Eck, T. F., Dubovik, O., and Slutsker, I.: Cloud screening and quality control algorithms for the AERONET database, *Remote Sens. Environ.*, 73, 337–349, 2000.

Streets, D. G., Gupta, S., Waldhoff, S. T., Wang, M. Q., Bond, T. C., and Bo, Y.: Black carbon emissions in China, *Atmos. Environ.*, 35, 4281–4296, 2001.

Su, X., Cao, J., Li, Z., Lin, M., and Wang, G.: Column-integrated aerosol optical properties during summer and autumn of 2012 in Xi'an, China, *Aerosol Air Qual. Res.*, 14, 850–861, 2014.

Tan, H., Wu, D., Deng, X., Bi, X., Li, F., and Deng, T.: Observation of aerosol optical depth over the Pearl River Delta, *Acta Scientiae Circumstantiae*, 29, 1146–1155, 2009 (in Chinese).

Tao, R., Che, H. Z., Chen, Q. L., Wang, Y. Q., Sun, J. Y., Zhang, X. C., Lu, S., Guo, J. P., Wang, H., and Zhang, X. Y.: Development of an integrating sphere calibration method for Cimel sunphotometers in China aerosol remote sensing network, *Particuology*, 13, 88–99, doi:10.1016/j.partic.2013.04.009, 2014.

Uchiyama, A., Yamazaki, A., Togawa, H., and Asano, J.: Characteristics of aeolian dust observed by sky-radiometer in the Intensive Observation Period 1 (IOP1), *J. Meteorol. Soc. Jpn.*, 83A, 291–305, 2005.

Wang, D. and Qiu, J.: The study of atmospheric aerosol optical properties in Takla-Makan desert in spring, *Chinese J. Atmos. Sci.*, 12, 75–81, 1988 (in Chinese).

Wang, J., Yang, S., Zhao, Q., and Cui, S.: Analyses of aerosol properties in Hefei based on polarization measurements of a sun photometer, *Int. J. Remote Sens.*, 33, 69–80, 2012.

**Ground-based  
aerosol climatology  
of China**

H. Che et al.

Title Page

Abstract

Introduction

Conclusions

References

Tables

Figures



Back

Close

Full Screen / Esc

Printer-friendly Version

Interactive Discussion



Wang, P., Che, H., Zhang, X., Song, Q., Wang, Y., Zhang, Z., Dai, X., and Yu, D.: Aerosol optical properties of regional background atmosphere in northeast China, *Atmos. Environ.*, 44, 4404–4412, doi:10.1016/j.atmosenv.2010.07.043, 2010.

Wang, X., Huang, J., Zhang, R., Chen, B., and Bi, J.: Surface measurements of aerosol properties over northwest China during ARM China 2008 deployment, *J. Geophys. Res.*, 115, D00K27, doi:10.1029/2009JD013467, 2010.

Wang, Z., Liu, D., Wang, Z., Wang, Y., Khatri, P., Zhou, J., Takamura, T., and Shi, G.: Seasonal characteristics of aerosol optical properties at the SKYNET Hefei site (31.90° N, 117.17° E) from 2007 to 2013, *J. Geophys. Res.-Atmos.*, 119, 6128–6139, doi:10.1002/2014JD021500, 2014.

Wehrli, C.: Calibration of filter radiometers for the GAW Aerosol Optical Depth Network at Jungfraujoch and Mauna Loa, in: *Proceedings of ARJ Workshop, SANW Congress, Davos, Switzerland*, 70–71, 2002.

Xia, X.: A closer looking at dimming and brightening in China during 1961–2005, *Ann. Geophys.*, 28, 1121–1132, doi:10.5194/angeo-28-1121-2010, 2010.

Xia, X. A., Chen, H. B., Wang, P. C., Zong, X. M., and Gouloub, P.: Aerosol properties and their spatial and temporal variations over north China in spring 2001, *Tellus B*, 57, 28–39, 2005.

Xia, X. A., Chen, H. B., Li, Z. Q., Wang, P. C., and Wang, J. K.: Significant reduction of surface solar irradiance induced by aerosols in a suburban region in northeastern China, *J. Geophys. Res.*, 112, 1–9, 2007.

Xiao, Z., Jiang, H., Chen, J., Wang, B., and Jiang, Z.: Monitoring the aerosol optical properties over Hangzhou using remote sensing data, *Acta Scientiae Circumstantiae*, 31, 1758–1767, 2011 (in Chinese).

Xie, Y., Zhang, Y., Xiong, X., Qu, J. J., and Che, H.: Validation of MODIS aerosol optical depth product over China using CARSNET measurements, *Atmos. Environ.*, 45, 5970–5978, 2011.

Xin, J., Wang, Y., Li, Z., Wang, P., Hao, W., Nordgren, B., Wang, S., Liu, G., Wang, L., Wen, T., Sun, Y., and Hu, B.: Aerosol optical depth (AOD) and Angstrom exponent of aerosols observed by the Chinese Sun Hazemeter Network from August 2004 to September 2005, *J. Geophys. Res.*, 112, D05203, doi:10.1029/2006JD007075, 2007.

Yoon, S., Kim, S., Choi, S., and Choi, I.: Regional-scale relationships between aerosol and summer monsoon circulation, and precipitation over northeast Asia, *Asia Pac. J. Atmos. Sci.*, 46, 279–286, 2010.

**Ground-based  
aerosol climatology  
of China**

H. Che et al.

Title Page

Abstract

Introduction

Conclusions

References

Tables

Figures



Back

Close

Full Screen / Esc

Printer-friendly Version

Interactive Discussion



Zhang, J., Mao, J., and Wang, M.: Analysis of aerosol extinction characteristics in different areas of China, *Adv. Atmos. Sci.*, 19, 136–152, 2002.

Zhang, J., Chen, J., Xia, X., Che, H., Fan, X., Xie, Y., Chen, H., and Lu, D.: Heavy aerosol loading over the Bohai Bay as revealed by ground and satellite remote sensing, *Atmos. Environ.*, doi:10.1016/j.atmosenv.2015.03.048, in press, 2015.

Zhang, X. Y., Wang, Y. Q., Niu, T., Zhang, X. C., Gong, S. L., Zhang, Y. M., and Sun, J. Y.: Atmospheric aerosol compositions in China: spatial/temporal variability, chemical signature, regional haze distribution and comparisons with global aerosols, *Atmos. Chem. Phys.*, 12, 779–799, doi:10.5194/acp-12-779-2012, 2012.

Zhao, B., Wang, Q., Mao, J., and Qin, Y.: Study on remote sensing of aerosol optical depth and vapor, *Sci. China Ser. B*, 10, 951–962, 1983 (in Chinese).

Zhao, H., Che, H., Zhang, X., Ma, Y., Wang, Y., Wang, H., and Wang, Y.: Characteristics of visibility and particulate matter (PM) in an urban area of Northeast China, *Atmos. Poll. Res.*, 4, 427–434, doi:10.5094/APR.2013.049, 2013a.

Zhao, H., Che, H., Zhang, X., Ma, Y., Wang, Y., Wang, X., Liu, C., Hou, B., and Che, H.: Aerosol optical properties over urban and industrial region of northeast China by using ground-based sun-photometer measurement, *Atmos. Environ.*, 75, 270–278, 2013b.

Zhu, J., Liao, H., and Li, J.: Increases in aerosol concentrations over eastern China due to the decadal-scale weakening of the East Asian summer monsoon, *Geophys. Res. Lett.*, 39, L09809, doi:10.1029/2012GL051428, 2012.

Zhu, J., Che, H., Xia, X., Chen, H., Goloub, P., and Zhang, W.: Column-integrated aerosol optical and physical properties at a regional background atmosphere in North China Plain, *Atmos. Environ.*, 84, 54–64, doi:10.1016/j.atmosenv.2013.11.019, 2014.

**Table A1.** Site information for the 50 CARSNET sites used in this study.

No.	Site Name	Long.	Lat.	Alt.	Site information	Obs. days
Remote sites (4 sites)						
1	Akedala	47.12	87.97	562.0	55 km west of Fuhai county, Xinjiang province, and 250–300 km southeast of Kazakestan.	464
2	Lhasa	29.67	91.13	3663.0	In the center of Lhasa city, Qinghai-Xizang Plateau.	830
3	Mt. Walliguan	36.28	100.92	3810.0	In the east edge of Qinghai-Xizang Plateau, Qinghai Province, Global GAW station	470
4	Shangri-La	28.02	99.73	3583.0	12 km northeast of Shangri-La county (Diqing area, Yunnan province, China)	701
Rural sites near the northern and northwestern deserts of China (11 sites)						
5	Dunhuang	40.15	94.68	1139.0	1.5 km northeast of Dunhuang city, Gansu province; near Kumutage Desert of China	2370
6	Ejina	41.95	101.07	940.5	West of Inner-Mongolia Province, near Mongolia and Badanjinlin desert	2250
7	Hami	42.82	93.52	737.0	500 km east from Urumuqi, In Hami county, nearby the Gobi desert, Xinjiang Province	685
8	Hotan	37.13	79.93	1374.7	South edge of Taklamakan Desert, 1000 km south from Urumuqi, Xinjiang Province	612
9	Jiuquan	39.77	98.48	1477.3	5 km north of Jiuquan City, Gansu Province, nearby the Badanjinlin Desert	412
10	Minqin	38.63	103.08	1367.0	In Minqin county, east to Tenggelii desert and north to Badanjinlin Desert, Gansu Province	1435
11	Tazhong	39.00	83.67	1099.4	In the middle of Taklamakan Desert, Xinjiang Province	1984
12	Ulaite	41.57	108.52	1288.0	Northwest of Inner-Mongolia, but in grass desertification region	712
13	Xilinhot	43.95	116.12	1003.0	5 km southeast of Xilinhot City, Inner-Mongolia Province, and near Hunshandake sand-land	2228
14	Zhangbei	41.15	114.70	1093.4	40 km north of Zhangjiakou City Hebei Province, and near Hunshandake sand-land	219
15	Zhurhe	42.40	112.90	1152.0	In the middle of Inner Mongolia Province, and nearby Hunshandake sand-land	365
Rural sites on or near the Chinese Loess Plateau (4 sites)						
16	Dongsheng	39.83	109.98	1460.5	In the center of Erdos city, Inner Mongolia province.	234
17	Mt. Gaolan	36.00	103.85	2161.6	5 km north from Lanzhou city, Gansu province.	766
18	Yanan	36.60	109.50	958.5	2 km northeast of Yan'an city, Shaanxi Province	218
19	Yulin	38.43	109.20	1135.0	10 km north of Yulin city, Shaanxi province	451
Rural sites in eastern China (10 sites)						
20	Changde	29.17	111.70	565.0	18 km northwest from Changde city, Hunan province.	210
21	Dongtan	31.52	121.96	10.0	In the Chongmin Island, 30 km east of Shanghai city	374
22	Gucheng	39.13	115.80	45.2	Within area of rapid urbanization, 38 km southwest of Baoding city, Hebei province.	750
23	Huimin	37.48	117.53	11.7	100 km Northeast of Jinan City, Shandong Province	851
24	Lin'an	30.30	119.73	138.6	150 km northeast of Shanghai, and 50 km west of Hangzhou city, Zhejiang province	1029
25	Mt. Longfeng	44.73	127.60	330.5	In Wuchang county, 175 km northeast of Harbin city, Heilongjiang Province	1357
26	Mt. Tai	36.25	117.10	1591.0	At summit of Mt. Tai, middle of northern China Plain, Shandong Province	173
27	Shangdianzi	40.65	117.12	293.0	In Miyun county, 150 km northeast to Beijing city.	2042
28	Tongyu	44.42	122.87	151.0	In Tonyu county, west of Jilin Province	738
29	Yushe	37.07	112.98	1041.5	1.5 km east of Yushe county, Shanxi Province	1045
Urban sites (21 sites)						
30	Anshan	41.08	123.00	23.0	In the center of Anshan city, Liaoning province.	230
31	Beijing	39.80	116.47	31.3	In the southeast of Beijing center at city margin	1594
32	Benxi	41.32	123.78	183.0	In the center of Benxi city, Liaoning province.	376
33	Chengdu	30.65	104.03	496.0	In the center of Chengdu city, Sichuan province.	212
34	Dalian	38.90	121.63	91.5	Southeast of Dalian center at city margin, Liaoning Province	763
35	Datong	40.10	113.33	1067.3	9 km of Datong City, but within area of rapid urbanization, Shanxi Province	2269
36	Fushu	41.88	123.95	80.0	In the center of Fushu city, Liaoning province.	242
37	Hangzhou	30.23	120.17	42.0	In the center of Hangzhou city, Zhejiang province.	365
38	Hefei	31.98	116.38	92.0	In the center of Hefei city, Anhui province.	293
39	Kunming	25.01	102.65	1889.0	In the west region of Kunming city, Yunnan province	301
40	Lanzhou	36.05	103.88	1517.3	In the center of Lanzhou city, Gansu province.	2157
41	Nanjing	32.05	118.77	99.3	In the center of Nanjing city, Jiangsu province	128
42	Nanning	22.82	108.35	172.0	In Nanning city, Guangxi province	390
43	Panyu	23	113.35	145.0	In Panyu district of Guangzhou city, Guangdong Province	142
44	Pudong	31.22	121.55	14.0	In Pudong district of Shanghai city	317
45	Shenyang	41.77	123.50	60.0	In the center of Shenyang city, Liaoning province.	477
46	Tianjin	39.10	117.17	3.3	In the center of Tianjin City.	1452
47	Urumqi	43.78	87.62	935.0	In the center of Urumuqi city, Xijiang province	1624
48	Xi'an	34.43	108.97	363.0	20 km north of center of Xi'an city, but within Jing River Industrial District, Shaanxi province	569
49	Yinchuan	38.48	106.22	1111.5	In the center of Yinchuan city, Ningxia province.	273
50	Zhengzhou	34.78	113.68	99.0	In the center of Zhengzhou city, Henan province.	915



**Table A2.** Data for Figs. 2 and 3.

No.	Name	AOD				Alpha					
		Annual	Spring	Summer	Fall	Winter	Annual	Spring	Summer	Fall	Winter
1	Akedala	0.20	0.21	0.23	0.15	0.22	1.13	0.92	1.12	1.13	1.33
2	Anshan	0.70	0.77	0.82	0.62	0.58	0.79	0.83	0.85	0.96	0.96
3	Beijing	0.76	0.83	0.92	0.63	0.65	1.01	0.85	1.15	1.08	0.97
4	Benxi	0.85	0.82	1.03	0.65	1.03	0.52	0.62	0.61	0.76	0.59
5	Changde	0.59	0.63	0.44	0.61	0.69	1.18	0.89	1.31	1.35	1.18
6	Chengdu	0.98	1.08	0.99	0.68	1.16	1.09	0.96	1.17	1.14	1.09
7	Dalian	0.54	0.64	0.68	0.50	0.40	1.13	1.12	1.24	1.27	0.98
8	Datong	0.51	0.49	0.57	0.44	0.52	0.84	0.68	0.93	0.89	0.87
9	Dongsheng	0.46	0.50	0.61	0.38	0.34	0.79	0.56	1.03	0.78	0.79
10	Dongtan	0.62	0.62	0.67	0.49	0.69	1.13	1.08	1.24	1.11	1.11
11	Dunhuang	0.32	0.48	0.32	0.21	0.28	0.46	0.29	0.40	0.55	0.59
12	Ejina	0.25	0.36	0.27	0.18	0.18	0.57	0.37	0.56	0.68	0.67
13	Fushu	0.49	0.49	0.55	0.47	0.44	0.84	0.85	0.93	0.94	0.94
14	Gucheng	0.70	0.73	0.72	0.69	0.68	1.24	1.11	1.28	1.31	1.27
15	Hami	0.25	0.31	0.24	0.20	0.26	0.62	0.54	0.71	0.57	0.66
16	Hangzhou	1.01	1.07	0.88	1.02	1.07	1.24	1.17	1.24	1.31	1.24
17	Hefei	0.83	0.89	0.82	0.77	0.85	1.19	0.99	1.23	1.29	1.26
18	Hotan	0.61	0.75	0.75	0.37	0.51	0.22	0.09	0.10	0.30	0.48
19	Huimin	0.71	0.74	0.79	0.66	0.65	1.14	0.96	1.25	1.27	1.09
20	Jiuquan	0.31	0.43	0.29	0.21	0.30	0.50	0.39	0.48	0.49	0.65
21	Jurih	0.24	0.29	0.36	0.18	0.14	0.80	0.57	0.83	0.80	1.01
22	Kunming	0.41	0.53	0.57	0.35	0.18	1.24	1.33	0.98	1.19	1.48
23	Lanzhou	0.80	0.79	0.59	0.80	1.01	0.92	0.64	0.98	1.06	0.98
24	Lhasa	0.11	0.16	0.12	0.09	0.09	0.89	0.67	1.01	1.10	0.78
25	Lin'an	0.78	0.80	0.75	0.79	0.77	1.27	1.10	1.32	1.39	1.29
26	Minqin	0.39	0.46	0.44	0.35	0.29	0.54	0.37	0.51	0.58	0.68
27	Mt. Gaolan	0.46	0.55	0.41	0.43	0.46	0.78	0.59	0.86	0.85	0.83
28	Mt. Longfeng	0.34	0.40	0.34	0.29	0.31	1.38	1.32	1.44	1.42	1.35
29	Mt. Tai	0.33	0.36	0.51	0.29	0.17	1.05	0.74	1.16	1.14	1.18
30	Mt. Waliguan	0.14	0.21	0.17	0.09	0.09	0.59	0.34	0.75	0.72	0.54
31	Nanjing	0.89	0.90	1.24	0.69	0.73	1.24	1.03	1.32	1.35	1.28
32	Nanning	0.82	0.99	0.73	0.82	0.74	1.50	1.45	1.41	1.58	1.57
33	Panyu	0.78	0.96	0.53	0.81	0.81	1.36	1.37	1.30	1.42	1.35
34	Pudong	0.80	0.89	0.99	0.64	0.68	1.26	1.12	1.27	1.34	1.30
35	Shangdianzi	0.48	0.55	0.63	0.42	0.33	1.11	0.96	1.20	1.17	1.10
36	Shangri-La	0.11	0.13	0.15	0.09	0.06	1.26	1.16	1.28	1.39	1.19
37	Shenyang	0.76	0.80	0.86	0.59	0.79	0.88	0.90	0.98	1.05	0.84
38	Tazhong	0.54	0.81	0.66	0.34	0.33	0.29	0.10	0.15	0.38	0.51
39	Tianjin	0.74	0.78	0.89	0.67	0.64	1.08	0.92	1.17	1.16	1.07
40	Tongyu	0.26	0.33	0.32	0.23	0.16	1.35	1.14	1.20	1.26	1.79
41	Ulate	0.28	0.34	0.36	0.21	0.23	0.75	0.64	0.86	0.73	0.77
42	Urumqi	0.47	0.48	0.27	0.39	0.73	0.96	0.81	0.94	1.01	1.08
43	Xi'an	0.90	0.89	0.98	0.83	0.90	0.89	0.70	1.02	0.94	0.92
44	Xilinhot	0.26	0.32	0.33	0.19	0.19	0.79	0.75	0.88	0.79	0.75
45	Yanan	0.37	0.38	0.41	0.37	0.34	0.89	0.63	1.01	1.04	0.87
46	Yinchuan	0.52	0.56	0.53	0.49	0.50	0.87	0.66	0.98	0.90	0.93
47	Yulin	0.38	0.41	0.50	0.27	0.34	0.82	0.60	0.93	0.96	0.79
48	Yushe	0.58	0.57	0.77	0.49	0.48	1.02	0.79	1.19	1.09	1.04
49	Zhangbei	0.30	0.33	0.36	0.30	0.24	0.56	0.50	0.64	0.58	0.52
50	Zhengzhou	0.94	0.94	1.08	0.87	0.87	1.10	0.85	1.23	1.20	1.10

**Ground-based aerosol climatology of China**

H. Che et al.

[Title Page](#)

[Abstract](#) [Introduction](#)

[Conclusions](#) [References](#)

[Tables](#) [Figures](#)

[⏪](#) [⏩](#)

[◀](#) [▶](#)

[Back](#) [Close](#)

[Full Screen / Esc](#)

[Printer-friendly Version](#)

[Interactive Discussion](#)



**Table A3.** Data of Figs. 5–15: AOD.

Site	AOD	Jan	Feb	Mar	Apr	May	Jun	Jul	Aug	Sep	Oct	Nov	Dec
1 Akedala	Mean	0.16	0.28	0.24	0.21	0.17	0.20	0.33	0.15	0.16	0.12	0.16	0.20
	SD	0.15	0.19	0.15	0.09	0.05	0.12	0.29	0.07	0.14	0.06	0.16	0.09
2 Lhasa	Mean	0.08	0.12	0.15	0.18	0.14	0.13	0.12	0.11	0.10	0.08	0.08	0.08
	SD	0.02	0.09	0.05	0.08	0.06	0.05	0.06	0.03	0.03	0.03	0.02	0.02
3 Mt. Waliguan	Mean	0.09	0.13	0.24	0.23	0.18	0.18	0.19	0.16	0.12	0.10	0.06	0.05
	SD	0.07	0.08	0.19	0.16	0.10	0.09	0.06	0.06	0.06	0.04	0.03	0.04
4 Shangri-La	Mean	0.06	0.07	0.17	0.13	0.10	0.08	0.17	0.19	0.14	0.08	0.07	0.05
	SD	0.03	0.03	0.09	0.08	0.07	0.03	0.11	0.02	0.05	0.04	0.03	0.02
5 Ejina	Mean	0.18	0.21	0.34	0.39	0.35	0.29	0.26	0.27	0.23	0.16	0.14	0.16
	SD	0.10	0.15	0.26	0.30	0.31	0.29	0.19	0.24	0.22	0.16	0.08	0.10
6 Zhurihe	Mean	0.11	0.17	0.17	0.27	0.42	0.49	0.34	0.27	0.22	0.18	0.13	0.13
	SD	0.05	0.14	0.06	0.15	0.27	0.43	0.18	0.18	0.20	0.14	0.12	0.10
7 Hami	Mean	0.27	0.29	0.35	0.30	0.28	0.34	0.19	0.18	0.18	0.21	0.22	0.23
	SD	0.17	0.14	0.20	0.21	0.15	0.30	0.11	0.09	0.09	0.12	0.09	0.11
8 Xilinhot	Mean	0.22	0.18	0.26	0.33	0.39	0.39	0.32	0.28	0.23	0.18	0.16	0.18
	SD	0.17	0.08	0.18	0.22	0.26	0.30	0.23	0.20	0.19	0.12	0.09	0.14
9 Wulate	Mean	0.23	0.24	0.30	0.33	0.39	0.44	0.35	0.28	0.24	0.21	0.19	0.21
	SD	0.14	0.12	0.18	0.18	0.26	0.39	0.24	0.20	0.15	0.13	0.09	0.14
10 Zhangbei	Mean	0.18	0.20	0.25	0.32	0.41	0.45	0.27	0.35	0.32	0.27		0.33
	SD	0.12	0.14	0.13	0.12	0.21	0.26	0.13	0.29	0.21	0.15		0.41
11 Jiuquan	Mean	0.28	0.39	0.36	0.55	0.36	0.33	0.27	0.28	0.24	0.23	0.17	0.24
	SD	0.11	0.26	0.22	0.40	0.23	0.19	0.09	0.15	0.10	0.11	0.04	0.13
12 Dunhuang	Mean	0.26	0.33	0.48	0.55	0.41	0.35	0.34	0.25	0.23	0.21	0.20	0.25
	SD	0.17	0.20	0.33	0.41	0.24	0.22	0.23	0.19	0.12	0.11	0.09	0.14
13 Minqin	Mean	0.26	0.35	0.48	0.48	0.43	0.43	0.45	0.44	0.39	0.36	0.29	0.27
	SD	0.18	0.23	0.31	0.27	0.22	0.25	0.26	0.23	0.18	0.14	0.13	0.14
14 Tazhong	Mean	0.30	0.44	0.75	0.91	0.77	0.73	0.64	0.61	0.51	0.30	0.22	0.26
	SD	0.23	0.24	0.40	0.46	0.37	0.33	0.32	0.29	0.26	0.16	0.16	0.17
15 Hotan	Mean	0.45	0.71	0.71	0.74	0.81	0.72	0.72	0.81	0.60	0.43	0.31	0.37
	SD	0.27	0.42	0.43	0.45	0.48	0.43	0.48	0.39	0.36	0.28	0.12	0.10
16 Dongsheng	Mean	0.29	0.41	0.47	0.55	0.47	0.72	0.55	0.56	0.52	0.36	0.26	0.31
	SD	0.15	0.22	0.35	0.24	0.22	0.44	0.28	0.29	0.32	0.19	0.08	0.15
17 Yulin	Mean	0.33	0.42	0.39	0.45	0.39	0.49	0.49	0.54	0.37	0.21	0.23	0.26
	SD	0.27	0.26	0.28	0.26	0.15	0.29	0.28	0.29	0.27	0.14	0.20	0.18
18 Yan'an	Mean	0.38	0.38	0.35	0.43	0.38	0.44	0.39	0.39	0.46	0.39	0.25	0.26
	SD	0.24	0.24	0.16	0.24	0.17	0.27	0.18	0.20	0.35	0.26	0.11	0.12
19 Mt. Gaolan	Mean	0.45	0.55	0.58	0.59	0.49	0.42	0.40	0.41	0.46	0.45	0.38	0.38
	SD	0.21	0.24	0.28	0.26	0.22	0.17	0.19	0.18	0.20	0.14	0.12	0.21
20 Yushe	Mean	0.53	0.52	0.52	0.62	0.55	0.69	0.75	0.86	0.71	0.39	0.37	0.40
	SD	0.39	0.34	0.32	0.34	0.32	0.42	0.37	0.42	0.46	0.26	0.30	0.33
21 Changde	Mean	0.82	0.73	0.82	0.58	0.49	0.45	0.40	0.47	0.70	0.56	0.57	0.51
	SD	0.35	0.26	0.47	0.23	0.24	0.24	0.21	0.22	0.37	0.44	0.24	0.30
22 Mt. Longfeng	Mean	0.32	0.31	0.32	0.46	0.41	0.42	0.30	0.30	0.27	0.32	0.29	0.30
	SD	0.22	0.22	0.24	0.29	0.21	0.29	0.23	0.23	0.25	0.26	0.20	0.21
23 Mt. Tai	Mean	0.15	0.28	0.28	0.37	0.42	0.58	0.51	0.43	–	0.15	0.16	0.09
	SD	0.14	0.20	0.24	0.23	0.19	0.34	0.31	0.22	–	0.08	0.19	0.05
24 Dongtan	Mean	0.64	0.83	0.70	0.64	0.51	0.67	0.58	0.78	0.40	0.44	0.62	0.59
	SD	0.37	0.43	0.32	0.22	0.19	0.50	0.45	0.39	0.21	0.23	0.30	0.27
25 Shangdianzi	Mean	0.32	0.37	0.49	0.57	0.58	0.72	0.56	0.60	0.51	0.43	0.34	0.31
	SD	0.35	0.39	0.45	0.43	0.39	0.59	0.51	0.45	0.45	0.41	0.35	0.30

Title Page

Abstract Introduction

Conclusions References

Tables Figures

◀ ▶

◀ ▶

Back Close

Full Screen / Esc

Printer-friendly Version

Interactive Discussion



Table A3. Continued.

Site	AOD	Jan	Feb	Mar	Apr	May	Jun	Jul	Aug	Sep	Oct	Nov	Dec
26 Huimin	Mean	0.64	0.72	0.72	0.81	0.71	0.90	0.78	0.70	0.68	0.69	0.62	0.61
	SD	0.32	0.32	0.36	0.29	0.29	0.31	0.31	0.33	0.37	0.39	0.32	0.35
27 Gucheng	Mean	0.66	0.77	0.65	0.77	0.76	0.81	0.76	0.59	0.79	0.64	0.62	0.63
	SD	0.45	0.47	0.45	0.45	0.48	0.53	0.46	0.34	0.46	0.48	0.45	0.38
28 Lin'an	Mean	0.83	0.84	0.81	0.81	0.78	0.96	0.58	0.72	0.90	0.82	0.65	0.65
	SD	0.33	0.30	0.29	0.31	0.29	0.32	0.34	0.32	0.34	0.35	0.29	0.29
29 Tongyu	Mean	0.18	0.13	0.21	0.35	0.44	0.44	0.32	0.20	0.17	0.36	0.15	0.18
	SD	0.16	0.06	0.19	0.33	0.44	0.42	0.26	0.14	0.14	0.34	0.13	0.18
30 Urumqi	Mean	0.71	0.85	0.63	0.44	0.35	0.27	0.28	0.26	0.30	0.35	0.53	0.65
	SD	0.37	0.40	0.31	0.20	0.21	0.13	0.14	0.10	0.13	0.15	0.28	0.37
31 Datong	Mean	0.55	0.50	0.44	0.51	0.53	0.53	0.57	0.61	0.52	0.40	0.42	0.50
	SD	0.32	0.31	0.25	0.26	0.32	0.37	0.41	0.37	0.33	0.22	0.20	0.27
32 Yinchuan	Mean	0.56	0.42	0.68	0.47	0.52	0.48	0.47	0.64	0.47	0.43	0.56	0.51
	SD	0.28	0.24	0.30	0.17	0.17	0.22	0.22	0.16	0.19	0.14	0.27	0.24
33 Dalian	Mean	0.36	0.44	0.55	0.63	0.60	0.67	0.74	0.62	0.55	0.51	0.43	0.41
	SD	0.25	0.32	0.37	0.36	0.24	0.34	0.41	0.29	0.42	0.36	0.33	0.33
34 Tianjin	Mean	0.60	0.75	0.75	0.79	0.81	1.00	0.84	0.82	0.70	0.68	0.62	0.56
	SD	0.46	0.49	0.49	0.45	0.44	0.57	0.49	0.49	0.44	0.48	0.39	0.37
35 Beijing	Mean	0.69	0.69	0.81	0.86	0.81	1.10	0.83	0.83	0.64	0.63	0.63	0.58
	SD	0.51	0.47	0.58	0.49	0.50	0.48	0.54	0.49	0.51	0.53	0.46	0.45
36 Nanjing	Mean	0.77	0.72	1.20	1.02	0.75	0.60	0.67	0.91	0.79	1.04	0.63	0.74
	SD	0.24	0.22	0.33	0.40	0.29	0.30	0.39	0.52	0.34	0.51	0.28	0.27
37 Lanzhou	Mean	1.03	0.88	0.88	0.81	0.68	0.56	0.59	0.63	0.68	0.78	0.93	1.13
	SD	0.31	0.30	0.37	0.29	0.23	0.16	0.22	0.23	0.22	0.21	0.30	0.34
38 Xi'an	Mean	0.86	1.07	1.02	0.81	0.83	0.81	0.97	1.17	0.86	0.83	0.80	0.77
	SD	0.49	0.42	0.32	0.31	0.34	0.34	0.34	0.43	0.38	0.41	0.39	0.33
39 Zhengzhou	Mean	0.87	1.04	1.00	0.91	0.90	1.08	1.00	1.14	0.97	0.91	0.74	0.70
	SD	0.52	0.47	0.44	0.45	0.51	0.49	0.40	0.45	0.50	0.46	0.40	0.42
40 Chengdu	Mean	1.09	1.24	1.30	1.07	0.87	0.88	0.89	1.20	0.74	0.50	0.79	1.16
	SD	0.38	0.49	0.40	0.39	0.37	0.30	0.51	0.38	0.33	0.19	0.29	0.36
41 Hangzhou	Mean	1.08	1.15	1.23	1.03	0.94	1.02	0.78	0.84	1.02	1.08	0.95	0.98
	SD	0.50	0.39	0.47	0.55	0.34	0.68	0.69	0.48	0.48	0.55	0.44	0.38
42 Pudong	Mean	0.50	0.90	0.67	0.97	1.04	1.26	0.90	0.81	0.63	0.69	0.60	0.65
	SD	0.27	0.35	0.34	0.31	0.59	0.61	0.53	0.55	0.40	0.34	0.30	0.37
43 Hefei	Mean	0.81	0.89	1.03	0.71	0.92	1.15	0.72	0.59	0.75	0.76	0.80	
	SD	0.22	0.26	0.28	0.25	0.21	0.18	0.34	0.24	0.25	0.18	0.40	
44 Kuming	Mean	0.20	0.19	0.62	0.48	0.49	0.45	0.46	0.78	0.65	0.25	0.15	0.16
	SD	0.09	0.09	0.28	0.29	0.26	0.27	0.27	0.42	0.48	0.17	0.08	0.15
45 Panyu	Mean	0.77	1.08	1.22	0.98	0.67	0.60	0.46	0.53	0.91	0.86	0.66	0.58
	SD	0.25	0.28	0.36	0.32	0.26	0.18	0.35	0.34	0.42	0.41	0.25	0.30
46 Nanjing	Mean	0.73	0.72	1.01	0.84	0.85	0.98	1.19	1.55	0.64	0.60	0.82	0.73
	SD	0.26	0.46	0.68	0.18	0.42	0.21	0.48	0.49	0.17	0.31	0.24	0.29
47 Shenyang	Mean	1.07	0.71	0.78	0.89	0.90	1.01	0.66	0.61	0.54	0.62	0.51	
	SD	0.40	0.43	0.34	0.33	0.50	0.51	0.43	0.42	0.40	0.39	0.32	
48 Anshan	Mean	0.56	0.75	0.44	0.78	1.08	0.80	0.92	0.72	0.77	0.51	0.57	0.43
	SD	0.28	0.41	0.17	0.36	0.43	0.41	0.37	0.40	0.42	0.31	0.39	0.14
49 Benxi	Mean	1.03	0.81	0.75	0.91	1.12	1.13	0.84	0.82	0.67	0.46		
	SD	0.32	0.34	0.28	0.41	0.42	0.37	0.34	0.50	0.36	0.07		
50 Fushun	Mean	0.60	0.26	0.49	0.50	0.41	0.66	0.59	0.45	0.40	0.55	0.48	
	SD	0.42	0.13	0.21	0.31	0.22	0.41	0.44	0.39	0.18	0.33	0.25	

Title Page

Abstract Introduction

Conclusions References

Tables Figures

◀ ▶

◀ ▶

Back Close

Full Screen / Esc

Printer-friendly Version

Interactive Discussion



**Table A4.** Data of Figs. 5–15: Alpha.

Site	Alpha	Jan	Feb	Mar	Apr	May	Jun	Jul	Aug	Sep	Oct	Nov	Dec
1 Akedala	Mean	1.45	1.23	0.90	1.00	0.88	0.96	1.18	1.24	1.02	1.20	1.19	1.32
	SD	0.39	0.37	0.67	0.31	0.26	0.28	0.24	0.22	0.35	0.44	0.46	0.39
2 Lhasa	Mean	0.80	0.62	0.53	0.73	0.76	0.85	0.94	1.22	1.16	1.07	1.08	0.92
	SD	0.32	0.25	0.20	0.24	0.23	0.27	0.32	0.35	0.25	0.26	0.22	0.27
3 Mt. Waliguan	Mean	0.61	0.36	0.25	0.35	0.40	0.56	0.96	0.74	0.65	0.77	0.75	0.65
	SD	0.33	0.23	0.14	0.22	0.33	0.26	0.38	0.32	0.24	0.27	0.28	0.33
4 Shangri-La	Mean	1.16	1.22	1.20	1.19	1.09	1.27	1.49	1.08	1.34	1.50	1.33	1.20
	SD	0.36	0.33	0.37	0.33	0.41	0.39	0.27	0.29	0.39	0.44	0.41	0.44
5 Ejina	Mean	0.73	0.56	0.35	0.35	0.39	0.49	0.58	0.61	0.68	0.64	0.73	0.72
	SD	0.37	0.34	0.27	0.25	0.26	0.29	0.32	0.32	0.34	0.29	0.33	0.37
6 Zhurihe	Mean	1.08	0.80	0.48	0.42	0.80	0.87	0.87	0.73	0.75	0.70	0.94	1.15
	SD	0.28	0.40	0.19	0.30	0.45	0.35	0.35	0.51	0.36	0.38	0.44	0.30
7 Hami	Mean	0.86	0.51	0.39	0.50	0.72	0.68	0.75	0.71	0.71	0.55	0.45	0.62
	SD	0.25	0.24	0.27	0.37	0.45	0.35	0.30	0.29	0.34	0.28	0.28	0.25
8 Xilinhot	Mean	0.69	0.74	0.73	0.75	0.78	0.86	0.88	0.89	0.89	0.76	0.73	0.82
	SD	0.35	0.48	0.48	0.44	0.40	0.42	0.39	0.41	0.44	0.46	0.42	0.35
9 Wulate	Mean	0.86	0.62	0.53	0.48	0.92	0.89	0.88	0.81	0.74	0.71	0.74	0.84
	SD	0.36	0.27	0.28	0.24	0.44	0.45	0.47	0.42	0.42	0.31	0.37	0.36
10 Zhangbei	Mean	0.56	0.48	0.48	0.39	0.62	0.76	0.62	0.54	0.66	0.50	0.53	0.53
	SD	0.20	0.19	0.17	0.15	0.25	0.19	0.22	0.33	0.31	0.28	0.22	0.22
11 Jiuquan	Mean	0.67	0.59	0.40	0.31	0.46	0.51	0.47	0.46	0.37	0.47	0.65	0.68
	SD	0.25	0.39	0.24	0.29	0.30	0.33	0.26	0.25	0.12	0.18	0.17	0.24
12 Dunhuang	Mean	0.65	0.47	0.27	0.26	0.33	0.36	0.38	0.46	0.50	0.51	0.65	0.65
	SD	0.27	0.30	0.21	0.22	0.23	0.23	0.30	0.28	0.29	0.24	0.28	0.33
13 Minqin	Mean	0.84	0.54	0.36	0.35	0.39	0.44	0.57	0.53	0.57	0.57	0.61	0.66
	SD	0.36	0.31	0.25	0.21	0.26	0.23	0.30	0.25	0.35	0.32	0.41	0.40
14 Tazhong	Mean	0.61	0.36	0.12	0.10	0.10	0.11	0.15	0.17	0.21	0.36	0.56	0.57
	SD	0.32	0.29	0.08	0.06	0.07	0.07	0.09	0.11	0.09	0.19	0.27	0.34
15 Hotan	Mean	0.66	0.18	0.13	0.07	0.06	0.07	0.15	0.08	0.11	0.20	0.39	0.59
	SD	0.26	0.13	0.14	0.07	0.06	0.07	0.13	0.06	0.07	0.10	0.16	0.20
16 Dongsheng	Mean	0.87	0.69	0.50	0.44	0.74	0.91	0.98	1.21	0.88	0.73	0.72	0.81
	SD	0.20	0.27	0.27	0.33	0.30	0.29	0.28	0.39	0.35	0.30	0.29	0.25
17 Yulin	Mean	0.98	0.59	0.59	0.67	0.54	0.64	0.92	1.25	1.02	0.93	0.93	0.80
	SD	0.37	0.22	0.31	0.32	0.26	0.36	0.35	0.23	0.33	0.29	0.27	0.30
18 Yan'an	Mean	1.04	0.65	0.63	0.60	0.65	1.05	0.97	1.01	1.14	0.97	1.01	0.91
	SD	0.21	0.28	0.23	0.28	0.27	0.24	0.35	0.15	0.25	0.25	0.23	0.29
19 Mt. Gaolan	Mean	0.94	0.77	0.64	0.57	0.56	0.84	0.88	0.87	0.79	0.91	0.86	0.77
	SD	0.31	0.31	0.30	0.28	0.30	0.40	0.38	0.31	0.29	0.26	0.36	0.32
20 Yushe	Mean	1.05	1.04	0.78	0.76	0.82	1.11	1.20	1.25	1.20	1.04	1.02	1.01
	SD	0.27	0.27	0.31	0.34	0.34	0.29	0.23	0.26	0.30	0.26	0.26	0.34
21 Changde	Mean	1.36	1.26	0.96	0.79	0.93	1.28	1.27	1.38	1.40	1.30	1.36	0.93
	SD	0.12	0.20	0.39	0.25	0.29	0.11	0.27	0.30	0.16	0.24	0.20	0.23
22 Mt. Longfeng	Mean	1.35	1.37	1.38	1.33	1.26	1.39	1.49	1.43	1.42	1.42	1.42	1.32
	SD	0.28	0.34	0.36	0.36	0.38	0.30	0.29	0.26	0.33	0.35	0.29	0.29
23 Mt. Tai	Mean	1.14	1.06	1.00	0.79	0.42	1.30	1.14	1.03	0.98	1.02	1.34	1.34
	SD	0.41	0.35	0.34	0.35	0.07	0.13	0.17	0.12	0.22	0.23	0.37	0.37
24 Dongtan	Mean	1.21	0.99	1.03	1.00	1.19	1.21	1.20	1.29	1.05	1.09	1.20	1.12
	SD	0.24	0.34	0.26	0.26	0.24	0.28	0.41	0.23	0.31	0.28	0.28	0.32
25 Shangdianzi	Mean	1.11	1.11	1.00	0.92	0.96	1.17	1.19	1.25	1.20	1.18	1.14	1.08
	SD	0.29	0.31	0.35	0.36	0.40	0.29	0.26	0.26	0.26	0.26	0.31	0.34

Title Page

Abstract Introduction

Conclusions References

Tables Figures

◀ ▶

◀ ▶

Back Close

Full Screen / Esc

Printer-friendly Version

Interactive Discussion



Table A4. Continued.

Site	Alpha	Jan	Feb	Mar	Apr	May	Jun	Jul	Aug	Sep	Oct	Nov	Dec
26 Huimin	Mean	1.16	1.09	0.97	0.96	0.95	1.19	1.25	1.32	1.33	1.22	1.26	1.03
	SD	0.20	0.28	0.31	0.32	0.35	0.21	0.16	0.17	0.26	0.22	0.15	0.32
27 Gucheng	Mean	1.36	1.23	1.10	1.16	1.06	1.22	1.27	1.34	1.26	1.32	1.35	1.22
	SD	0.26	0.30	0.37	0.34	0.32	0.31	0.24	0.30	0.34	0.27	0.26	0.40
28 Lin'an	Mean	1.27	1.30	1.13	0.97	1.18	1.24	1.26	1.44	1.39	1.38	1.40	1.29
	SD	0.26	0.28	0.27	0.32	0.30	0.33	0.43	0.30	0.25	0.28	0.21	0.33
29 Tongyu	Mean	1.92	1.90	1.34	1.04	1.05	1.21	1.27	1.13	1.08	1.26	1.44	1.55
	SD	0.66	0.55	0.39	0.38	0.39	0.32	0.33	0.29	0.37	0.42	0.47	0.64
30 Urumqi	Mean	1.08	1.02	0.91	0.74	0.78	0.85	1.05	0.92	0.91	0.99	1.13	1.15
	SD	0.23	0.23	0.33	0.37	0.39	0.31	0.32	0.29	0.29	0.25	0.24	0.28
31 Datong	Mean	0.91	0.80	0.68	0.63	0.72	0.86	0.94	0.99	0.98	0.84	0.86	0.90
	SD	0.19	0.25	0.28	0.32	0.34	0.33	0.25	0.25	0.27	0.25	0.24	0.22
32 Yinchuan	Mean	1.04	0.74	0.56	0.58	0.85	0.94	1.02	0.99	0.78	0.99	0.93	1.00
	SD	0.18	0.29	0.24	0.20	0.34	0.24	0.26	0.17	0.20	0.16	0.20	0.22
33 Dalian	Mean	0.95	0.96	0.94	1.04	1.11	1.21	1.25	1.26	1.24	1.31	1.26	1.04
	SD	0.27	0.33	0.30	0.37	0.35	0.27	0.22	0.31	0.35	0.23	0.22	0.31
34 Tianjin	Mean	1.07	1.06	0.93	0.88	0.96	1.15	1.14	1.24	1.18	1.13	1.17	1.08
	SD	0.30	0.28	0.30	0.33	0.34	0.25	0.25	0.26	0.30	0.28	0.32	0.33
35 Beijing	Mean	0.98	0.94	0.87	0.79	0.89	1.14	1.10	1.21	1.11	1.10	1.04	0.99
	SD	0.34	0.39	0.34	0.37	0.33	0.25	0.29	0.28	0.26	0.27	0.32	0.32
36 Nanjing	Mean	1.62	1.64	1.50	1.43	1.42	1.22	1.37	1.66	1.63	1.52	1.59	1.45
	SD	0.14	0.14	0.27	0.30	0.30	0.25	0.56	0.26	0.40	0.27	0.14	0.18
37 Lanzhou	Mean	1.03	0.86	0.65	0.58	0.70	0.92	1.02	1.01	1.03	1.04	1.11	1.05
	SD	0.22	0.31	0.32	0.29	0.27	0.26	0.23	0.22	0.19	0.19	0.23	0.22
38 Xi'an	Mean	0.97	0.88	0.73	0.59	0.79	0.88	1.03	1.15	0.99	1.00	0.83	0.91
	SD	0.30	0.32	0.36	0.33	0.36	0.39	0.35	0.29	0.32	0.32	0.28	0.27
39 Zhengzhou	Mean	1.15	1.15	0.82	0.82	0.91	1.18	1.25	1.26	1.24	1.25	1.12	0.99
	SD	0.26	0.26	0.34	0.32	0.34	0.25	0.21	0.23	0.25	0.27	0.32	0.36
40 Chengdu	Mean	1.11	1.04	0.93	0.98	0.97	1.11	1.19	1.21	1.05	1.11	1.24	1.10
	SD	0.20	0.16	0.32	0.35	0.28	0.22	0.20	0.14	0.25	0.28	0.16	0.17
41 Hangzhou	Mean	1.34	1.30	1.21	1.09	1.22	1.27	1.18	1.29	1.33	1.38	1.22	1.08
	SD	0.14	0.21	0.22	0.20	0.28	0.20	0.23	0.19	0.23	0.15	0.27	0.38
42 Pudong	Mean	1.37	1.27	1.04	1.14	1.19	1.23	1.31	1.28	1.24	1.41	1.38	1.26
	SD	0.24	0.22	0.30	0.25	0.32	0.23	0.29	0.23	0.52	0.17	0.14	0.31
43 Hefei	Mean	1.30	1.22	0.94	0.89	1.14	1.19	1.14	1.35	1.38	1.37	1.13	1.40
	SD	0.22	0.26	0.28	0.25	0.21	0.18	0.34	0.24	0.25	0.18	0.40	0.40
44 Kuming	Mean	1.55	1.69	1.52	1.32	1.14	0.98	0.90	1.06	1.00	1.32	1.24	1.21
	SD	0.29	0.19	0.17	0.18	0.27	0.36	0.47	0.23	0.43	0.16	0.24	0.25
45 Panyu	Mean	1.35	1.37	1.42	1.30	1.39	1.49	1.14	1.26	1.45	1.48	1.32	1.34
	SD	0.05	0.04	0.12	0.21	0.18	0.13	0.34	0.26	0.19	0.11	0.11	0.17
46 Nanjing	Mean	1.29	1.18	1.09	1.01	0.99	1.27	1.35	1.34	1.34	1.37	1.34	1.36
	SD	0.17	0.33	0.23	0.17	0.38	0.09	0.14	0.20	0.13	0.14	0.10	0.16
47 Shenyang	Mean	0.48	0.84	0.79	0.69	0.87	0.73	0.94	1.05	1.11	1.16	1.07	1.07
	SD	0.17	0.45	0.31	0.28	0.25	0.27	0.26	0.23	0.29	0.18	0.17	0.17
48 Anshan	Mean	0.72	0.95	0.83	0.59	0.29	0.75	0.79	0.66	1.09	1.06	0.88	0.87
	SD	0.51	0.26	0.24	0.23	0.15	0.30	0.18	0.32	0.20	0.23	0.31	0.23
49 Benxi	Mean	0.64	0.42	0.59	0.41	0.53	0.39	0.49	0.72	0.55	0.51	0.51	0.51
	SD	0.14	0.26	0.22	0.14	0.26	0.21	0.29	0.21	0.35	0.23	0.15	0.15
50 Fushun	Mean	0.95	1.03	0.20	0.84	0.77	0.52	1.01	0.81	0.81	0.95	1.03	1.07
	SD	0.22	0.14	0.27	0.36	0.32	0.69	0.26	0.26	0.26	0.26	0.25	0.17

Ground-based aerosol climatology of China

H. Che et al.

Title Page

Abstract Introduction

Conclusions References

Tables Figures

◀ ▶

◀ ▶

Back Close

Full Screen / Esc

Printer-friendly Version

Interactive Discussion







## Ground-based aerosol climatology of China

H. Che et al.

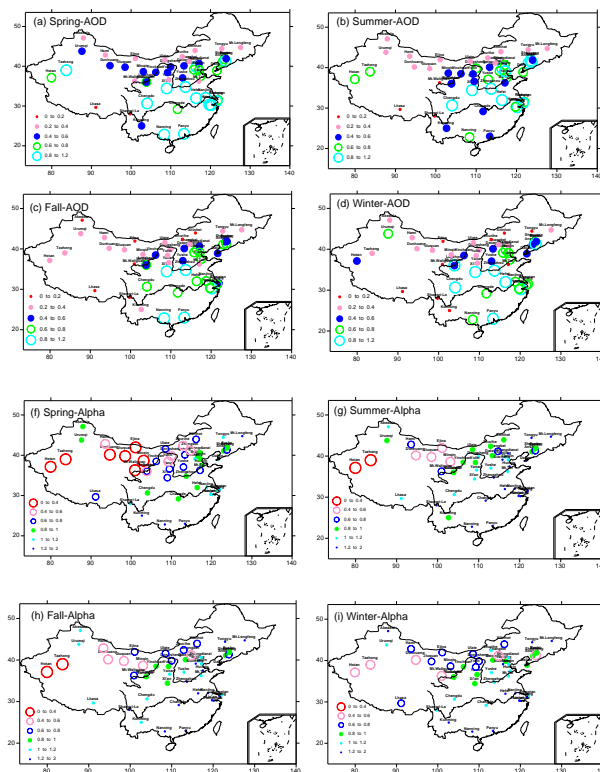


**Figure 3.** Seasonally stratified spatial distributions of AOD (**a**: spring; **b**: summer; **c**: fall; and **d**: winter) and Alpha (**e**: spring; **f**: summer; **g**: fall; and **h**: winter) based on CARSNET measurements.

Title Page

Abstract

Introduction

Conclusions

References

Tables

Figures



Back

Close

Full Screen / Esc

Printer-friendly Version

Interactive Discussion



## Ground-based aerosol climatology of China

H. Che et al.

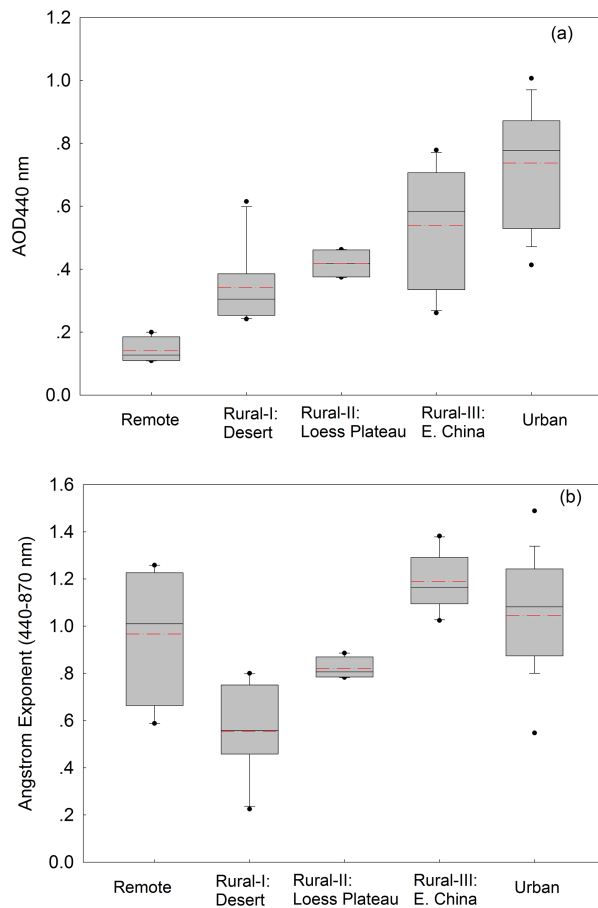


**Figure 4.** (a) AODs and (b) Alphas at remote, rural, and urban regions of China.

Title Page

Abstract Introduction

Conclusions References

Tables Figures

◀ ▶

◀ ▶

Back Close

Full Screen / Esc

Printer-friendly Version

Interactive Discussion



Ground-based  
aerosol climatology  
of China

H. Che et al.

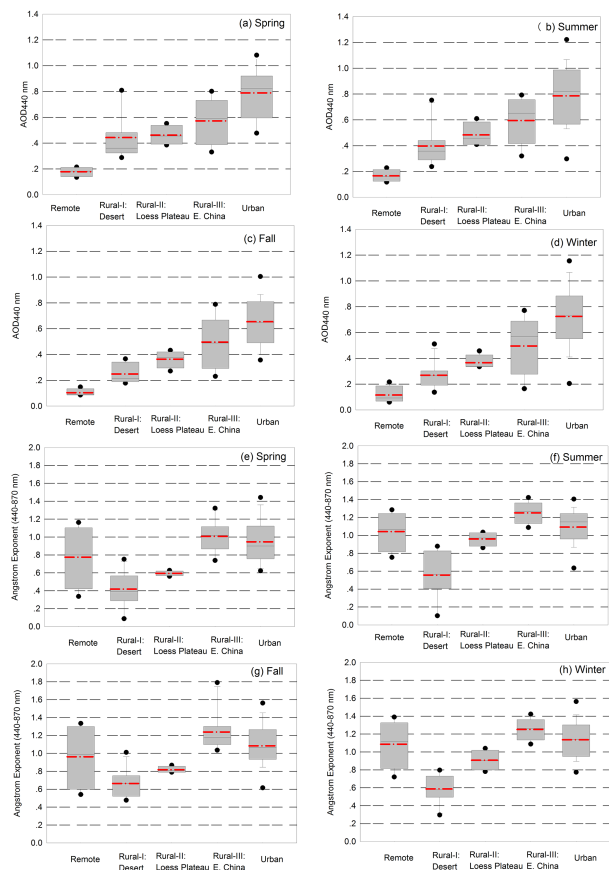


**Figure 5.** Seasonally averaged AODs (a–d) and Alphas (e–h) at remote, rural, and urban regions of China.

Title Page

Abstract Introduction

Conclusions References

Tables Figures

◀ ▶

◀ ▶

Back Close

Full Screen / Esc

Printer-friendly Version

Interactive Discussion



**Ground-based aerosol climatology of China**

H. Che et al.

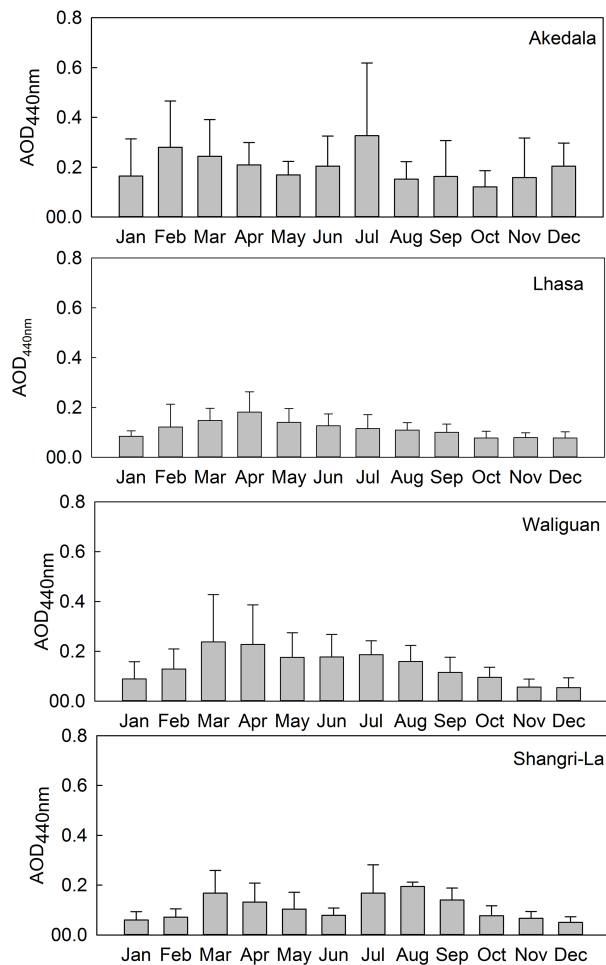


**Figure 6.** Monthly-averaged AODs at remote sites.

[Title Page](#)

[Abstract](#) | [Introduction](#)

[Conclusions](#) | [References](#)

[Tables](#) | [Figures](#)

[◀](#) | [▶](#)

[◀](#) | [▶](#)

[Back](#) | [Close](#)

[Full Screen / Esc](#)

[Printer-friendly Version](#)

[Interactive Discussion](#)



Ground-based  
aerosol climatology  
of China

H. Che et al.

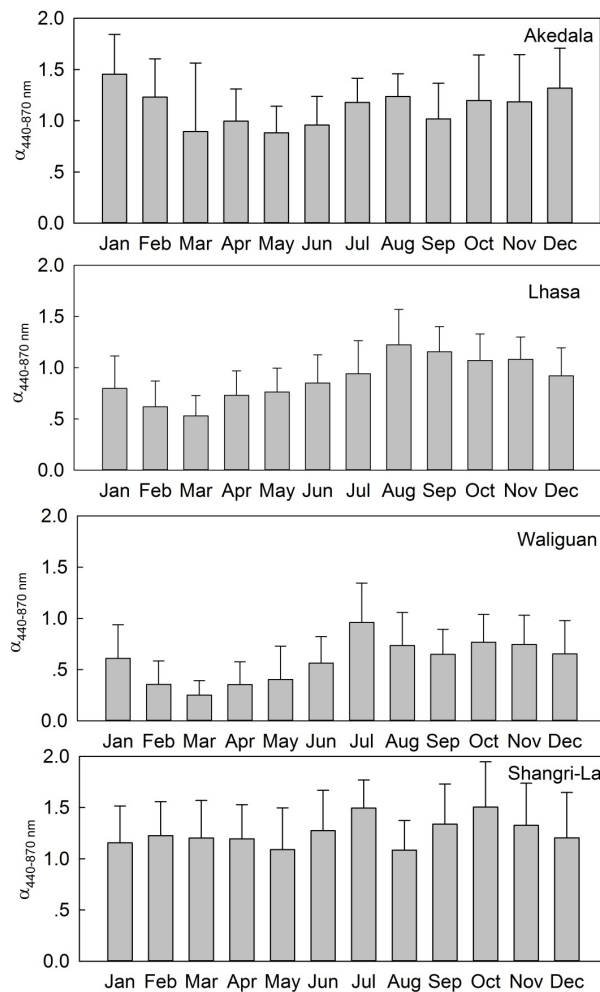
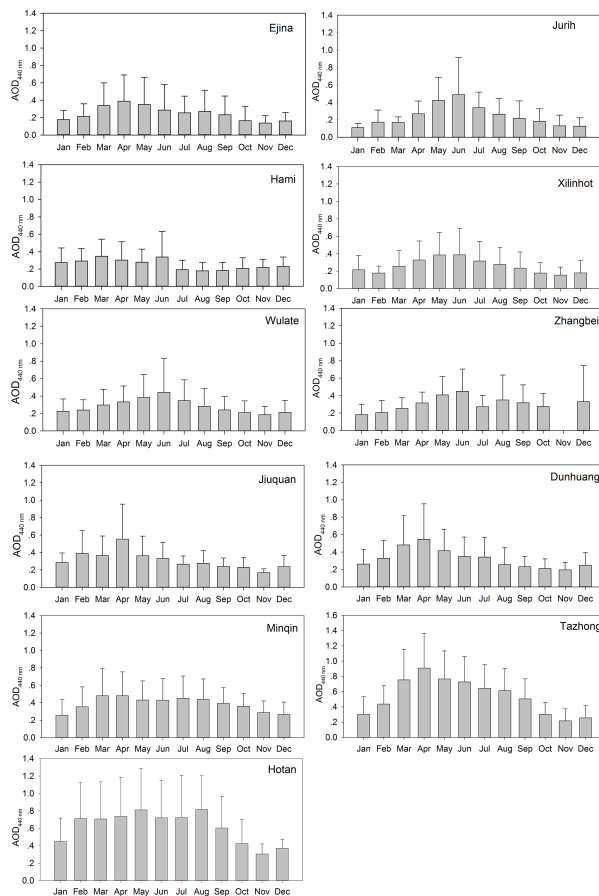


Figure 7. Monthly-averaged Alphas at remote sites.



**Ground-based aerosol climatology of China**

H. Che et al.



**Figure 8.** Monthly-averaged AODs at rural desert sites.

Title Page

Abstract Introduction

Conclusions References

Tables Figures

◀ ▶

◀ ▶

Back Close

Full Screen / Esc

Printer-friendly Version

Interactive Discussion



**Ground-based aerosol climatology of China**

H. Che et al.

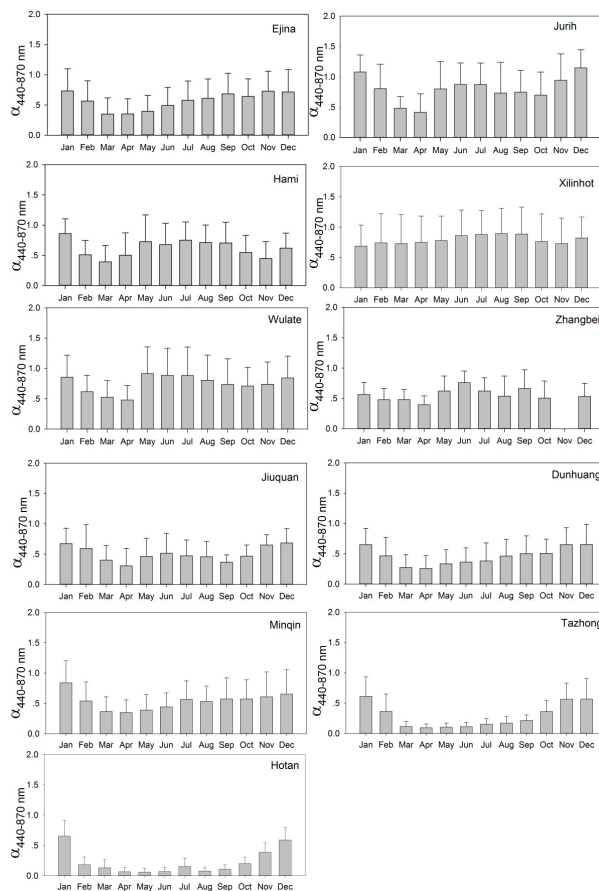


**Figure 9.** Monthly-averaged Alphas at rural desert sites.

Title Page

Abstract Introduction

Conclusions References

Tables Figures

◀ ▶

◀ ▶

Back Close

Full Screen / Esc

Printer-friendly Version

Interactive Discussion





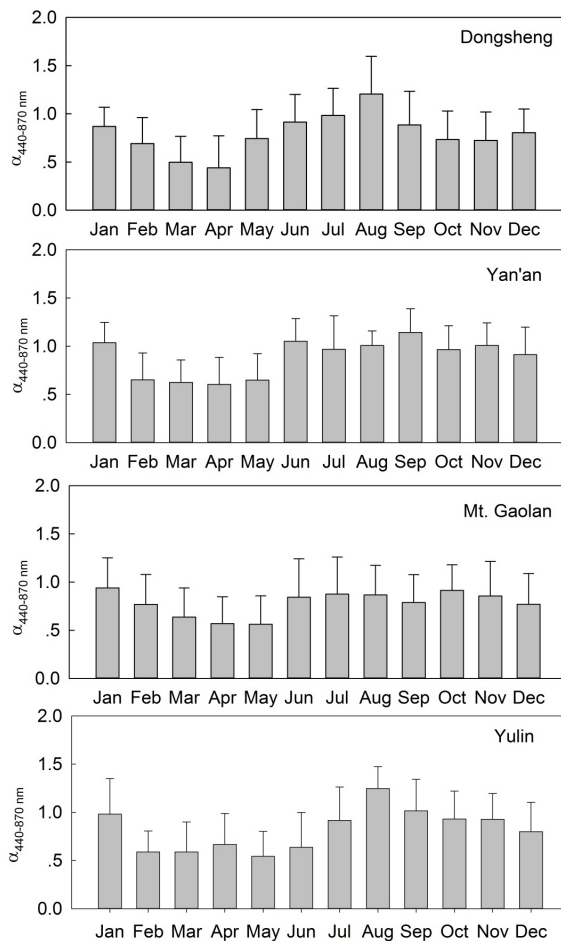


**Figure 11.** Monthly-averaged Alphas at rural Loess Plateau sites.

Title Page

Abstract Introduction

Conclusions References

Tables Figures

◀ ▶

◀ ▶

Back Close

Full Screen / Esc

Printer-friendly Version

Interactive Discussion



**Ground-based aerosol climatology of China**

H. Che et al.

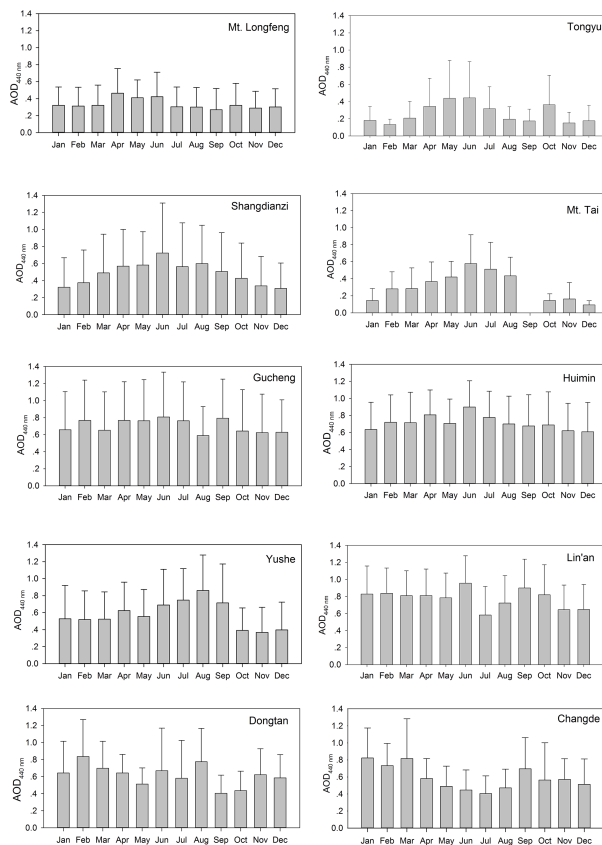


**Figure 12.** Monthly-averaged AODs at rural central and eastern China sites.

[Title Page](#)

[Abstract](#) | [Introduction](#)

[Conclusions](#) | [References](#)

[Tables](#) | [Figures](#)

[◀](#) | [▶](#)

[◀](#) | [▶](#)

[Back](#) | [Close](#)

[Full Screen / Esc](#)

[Printer-friendly Version](#)

[Interactive Discussion](#)



**Ground-based aerosol climatology of China**

H. Che et al.

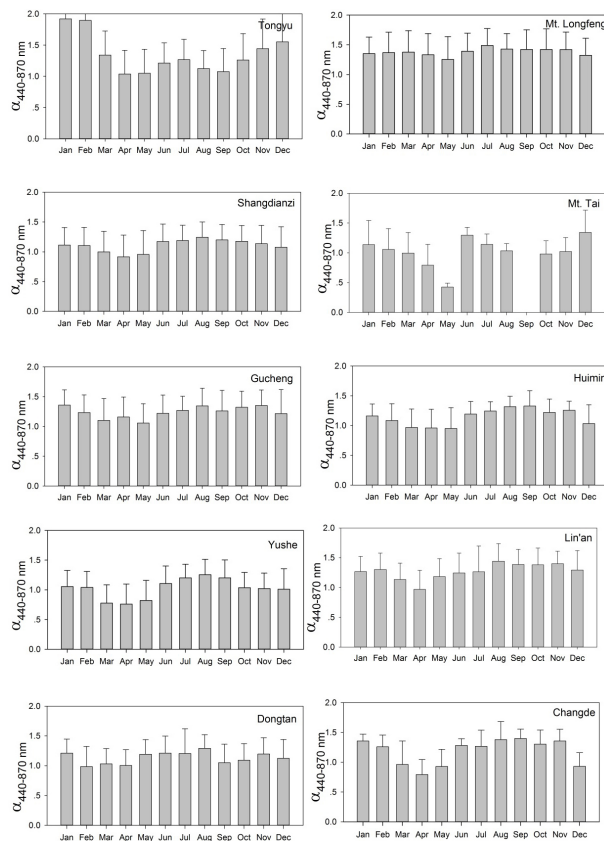


**Figure 13.** Monthly-averaged Alphas at rural central and eastern China sites.

[Title Page](#)  
[Abstract](#)   [Introduction](#)  
[Conclusions](#)   [References](#)  
[Tables](#)   [Figures](#)  
◀   ▶  
◀   ▶  
[Back](#)   [Close](#)  
[Full Screen / Esc](#)  
[Printer-friendly Version](#)  
[Interactive Discussion](#)



Ground-based aerosol climatology of China

H. Che et al.

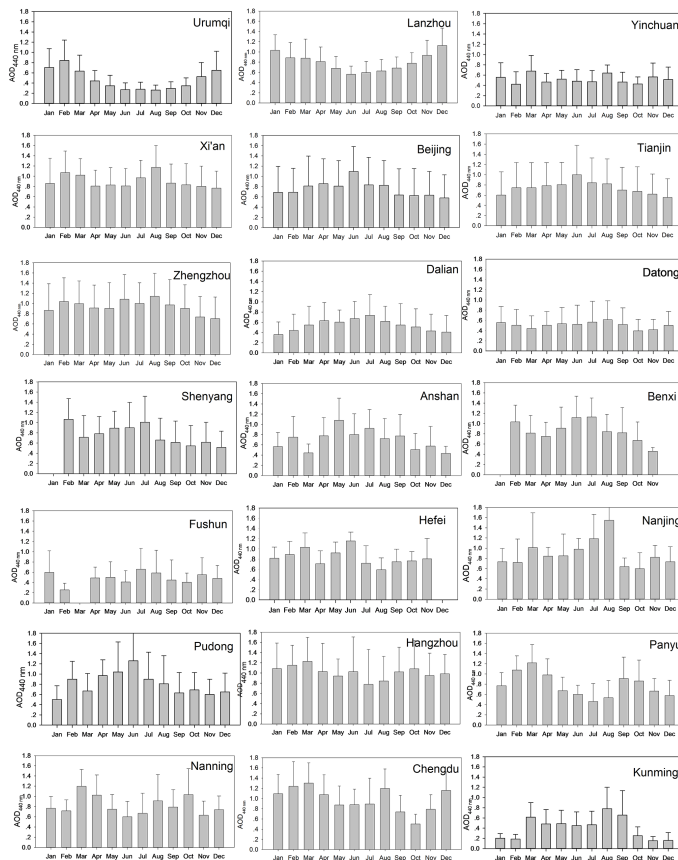


Figure 14. Monthly-averaged AODs at urban sites.

Title Page

Abstract Introduction

Conclusions References

Tables Figures

◀ ▶

◀ ▶

Back Close

Full Screen / Esc

Printer-friendly Version

Interactive Discussion



Ground-based aerosol climatology of China

H. Che et al.

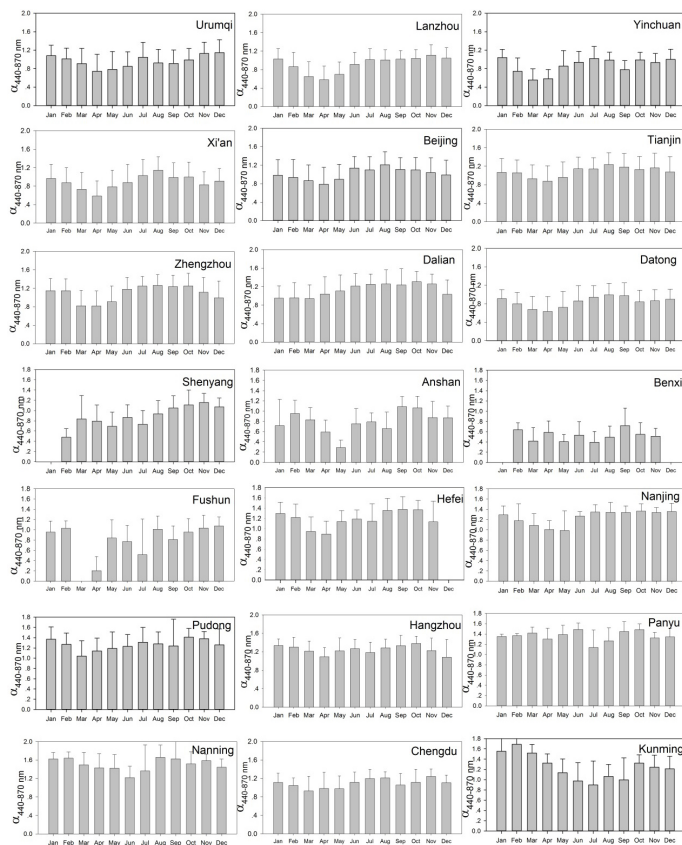


Figure 15. Monthly-averaged Alphas at urban sites.

Title Page

Abstract Introduction

Conclusions References

Tables Figures

◀ ▶

◀ ▶

Back Close

Full Screen / Esc

Printer-friendly Version

Interactive Discussion



## Ground-based aerosol climatology of China

H. Che et al.

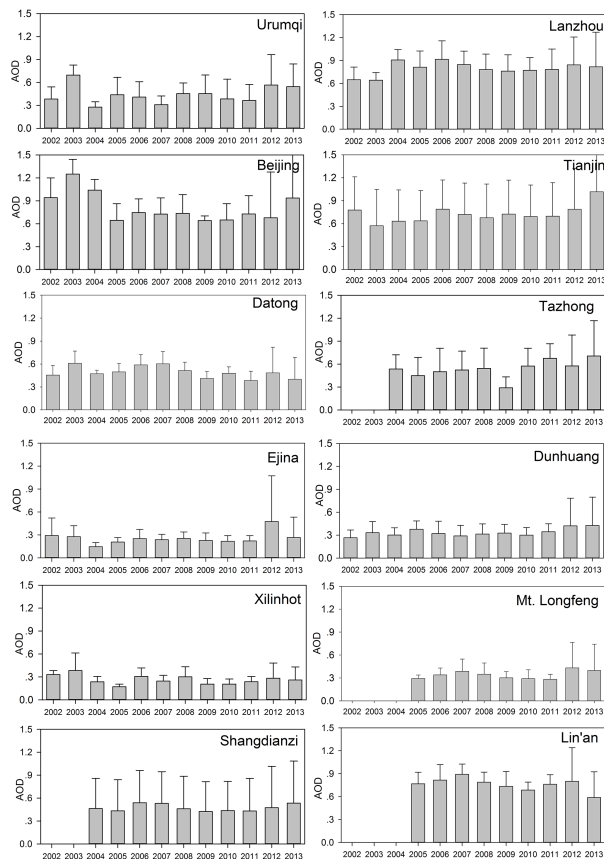


**Figure 16.** Annually-averaged AODs for the 12 long-term CARSNET sites.

[Title Page](#)  
[Abstract](#)   [Introduction](#)  
[Conclusions](#)   [References](#)  
[Tables](#)   [Figures](#)  
[◀](#)   [▶](#)  
[◀](#)   [▶](#)  
[Back](#)   [Close](#)  
[Full Screen / Esc](#)  
[Printer-friendly Version](#)  
[Interactive Discussion](#)



